ORGANOMETALLICS

pubs.acs.org/Organometallics Article

Is the Electrophilicity of the Metal Nitrene the Sole Predictor of Metal-Mediated Nitrene Transfer to Olefins? Secondary Contributing Factors as Revealed by a Library of High-Spin Co(II) Reagents

Anshika Kalra, Vivek Bagchi, Patrina Paraskevopoulou, Purak Das, Lin Ai, Yiannis Sanakis, Grigorios Raptopoulos, Sudip Mohapatra, Amitava Choudhury, Zhicheng Sun, Thomas R. Cundari,* and Pericles Stavropoulos*

Cite This: *Organometallics* 2021, 40, 1974–1996 Read Online

ACCESS | Metrics & More | Article Recommendations | Supporting Information

ABSTRACT: Recent research has highlighted the key role played by the electron affinity of the active metal-nitrene/imido oxidant as the driving force in nitrene additions to olefins to afford valuable aziridines. The present work showcases a library of Co(II) reagents that, unlike the previously examined Mn(II) and Fe(II) analogues, demonstrate reactivity trends in olefin aziridinations that cannot be solely explained by the electron affinity criterion. A family of Co(II) catalysts (17 members) has been synthesized with the assistance of a trisphenylamido-amine scaffold decorated by various alkyl, aryl, and acyl groups attached to the equatorial amidos. Single-crystal X-ray diffraction analysis, cyclic voltammetry and EPR data reveal that the high-spin Co(II) sites ($S = 3/2$) feature a minimal [N_3N] coordination and span a range of 1.4 V in redox potentials. Surprisingly, the Co(II)-mediated aziridination of styrene demonstrates reactivity patterns that deviate from those anticipated by the relevant electrophilicities of the putative metal nitrenes. The representative L^4Co catalyst ($-COCMe_3$ arm) is operating faster than the L^8Co analogue ($-COCF_3$ arm), in spite of diminished metal-nitrene electrophilicity. Mechanistic data (Hammett plots, KIE, stereocontrol studies) reveal that although both reagents follow a two-step reactivity path (turnover-limiting metal-nitrene addition to the C_b atom of styrene, followed by product-determining ring-closure), the L^4Co catalyst is associated with lower energy barriers in both steps. DFT calculations indicate that the putative [L^4Co]NTs and [L^8Co]NTs species are electronically distinct, inasmuch as the former exhibits a single-electron oxidized ligand arm. In addition, DFT calculations suggest that including London dispersion corrections for L^4Co (due to the polarizability of the *tert*-Bu substituent) can provide significant stabilization of the turnover-limiting transition state. This study highlights how small ligand modifications can generate stereoelectronic variants that in certain cases are even capable of overriding the preponderance of the metal-nitrene electrophilicity as a driving force.

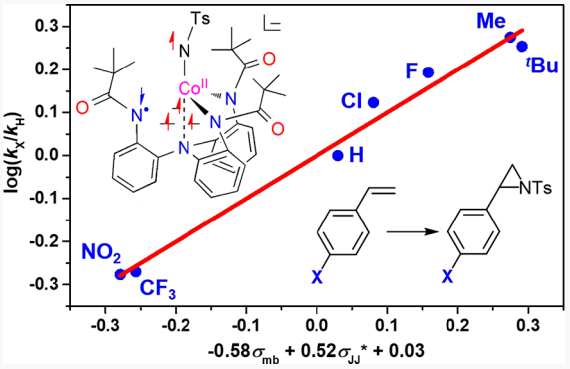

INTRODUCTION

The role of aziridines[1] as intermediates and end products of synthetic and biological chemistry is hard to overstate. Not only do aziridines afford avenues for further structural development by taking advantage of the energetic content and stereochemical disposition of their strained three-atom ring (ring opening, expansion, or rearrangement),[2] but also they constitute valuable functionalities in the framework of several natural products possessing antibiotic or antineoplastic activities.[3] In addition to the central role exercised by aziridines as fine chemicals and pharmaceutical agents,[4] their contribution to the chemistry of materials has been increasingly recognized,[5] especially as key entities for the development and postmodification of polymeric scaffolds.

Synthetic protocols for the generation of aziridines abound, but largely rely on three major methodologies. The cyclization of 1,2-amino precursors constitutes a traditional approach that has been more recently complemented by addition of either C_1 sources to imines or electrophilic N_1 donors to alkenes.[6] The latter "$C_2 + N_1$" addition is extensively implemented due to its operational simplicity and availability of a wide range of suitable

Received: May 1, 2021
Published: June 4, 2021

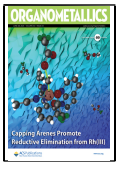

https://doi.org/10.1021/acs.organomet.1c00267
Organometallics 2021, 40, 1974–1996

substrates and catalysts. The N_1 donors encompass a variety of nitrene/nitrenoid precursor oxidants such as iminoiodanes (ArI=NR),[7] haloamines (RNNaX, X = Cl, Br),[8] *O*/*N*-substituted hydroxylamines and *N*-tosyloxycarbamates (RN(X)−OR′, X = H, leaving group)[9] or atom-economical organic azides (RN_3).[10] As opposed to oxo-transfer chemistry, the corresponding nitrene/nitrenoid transfer relies significantly on the choice of the attendant R group to control the electrophilicity of the active moiety and provide activated (R = SO_2R, CO_2R, COR, carbamoyl, sulfamoyl) or nonactivated aziridines (R = H, alkyl, aryl, silyl) with differential reactivity.[11]

A wide range of catalysts has been explored to influence reactivity and selectivity outcomes in nitrene transfer to alkenes, including several organocatalytic[12] and metal-mediated processes.[13] In the latter case, the presumptive and rather elusive metal-nitrene (M=NR) active species are entities with rich and variable stereoelectronic attributes, inherent and/or ligand induced, whose operation vis-à-vis olefinic substrates is a matter of intense investigation. The variety of transition metals employed, both from the first-row (Mn, Fe, Co, Ni, Cu)[14−22] and from the heavier platinum-group[23−25] and coinage elements,[26,27] coupled with a range of ancillary ligand frameworks (e.g., porphyrinoids, salens, bis-oxazolines, tetracarboxylate paddlewheels, trispyrazolyl-borates/methanes, polypyridines) is a testament to the vigorous activity in this field and that of the closely related C−H bond amination reactions.[28]

Among the late 3*d* transition elements, the case of cobalt is most intriguing, inasmuch as isolable or even putative Co=NR units have been invoked with a variety of oxidation states (from II to V), electronic ground-state spins (S = 0, 1/2, 1, 3/2, 2), and coordination numbers (from 2 to 5).[29] The most common configuration is that of diamagnetic Co(III) imidos (S = 0),[30] mostly supported by C_3 or C_2 symmetric ligands. In a handful of cases, open-shell spin-states were observed for Co(III) imidos, as for instance with (trispyrazolylborato)Co^{III}(NAd) (S = 1, at T > 280 K),[31] (dipyrrin)Co^{III}(NR) (S = 1 for R = Mes; S = 0 or 0 → 2 transition, for R = ^{t}Bu, 1-Ad, other alkyls),[32] $[(hmds)_2Co^{III}(N^tBu)]^-$ (S = 1; hmds = $N(SiMe_3)_2$),[33] and possibly bimetallic Zr(μ-NMes)Co^{III}(NMes) (S = 0 → 2 transition, near room temperature).[34] None of these compounds have been reported to mediate nitrene-transfer to alkenes. Observable reactivity includes (i) nitrene-transfer to carbon monoxide;[30g,31a,35] (ii) insertion of nitrene into ligand-derived carbene residues;[30e] (iii) formal hydrogen-atom abstraction from a ^{t}Bu or Mes ligand moiety by open-shell Co=NR, presumably generating an amido Co−NHR unit and a carbon centered radical; the latter can then recombine with the amido,[31a] dimerize,[31b] or generate a Co−C bond;[31b,32a] (iv) intramolecular C−H bond insertion into alkyl azides (source of imido), mediated by (dipyrrin)Co^{III}(NR), to generate substituted N-heterocycles;[32b,c] and (v) a rare instance of intermolecular hydrogen-atom abstraction from C−H bonds of various substrates with $BDE_{C-H} \leq 92$ kcal mol^{-1} by $[(hmds)_2Co^{III}(N^tBu)]^-$,[33] leading to the corresponding Co(II) amido; the amido can then react with another equivalent of substrate (C−H) to perform either proton transfer (frequently with the concomitant formation of Co^{II}−C organometallics) or formal hydrogen-atom abstraction via stepwise proton/electron transfer or direct HAT, giving rise to Co(I) and substrate dehydrogenation product. In several instances noted above, the carbophilic character of cobalt is notable as a product-determining factor.

Cobalt(II) imidos are more recent additions to the repertoire of cobalt reagents, and encompass both high-spin (S = 3/2)[36] and low-spin (S = 1/2)[37] cases as two- and four-coordinate compounds, respectively. The high-spin examples have been reported to perform nitrene-transfer to ethylene to afford RN=CH−CH_3, presumably due to a $[2\pi + 2\pi]$ activation mode. Similarly, certain C(sp)−H and Si−H bonds are activated not via H atom abstraction, but by means of $[2\pi + 2\sigma]$ interactions.[36b] On the other hand, the low-spin Co(II) imidos are unreactive versus alkenes, although they engage in nitrene-transfer and/or nitrene-exchange with O/S with respect to substrates such as CO, PMe_3, PhCHO, and CS_2.[37] Finally, two examples of high-valent Co(IV) and Co(V) bis-imido complexes ($[IMes]Co(NDipp)_2]^{0/+}$), possessing low-spin ground states of S = 1/2 and 0, respectively, proved to be rather unreactive.[38] The open-shell Co(IV) congener is the only one that exhibits intramolecular nitrene C−H insertion into the *o*-Me group of the Mes residue, possibly via an *ortho*-cobaltation intermediate (Co−C).[29]

Whereas the catalytic formation of new C−N bonds by means of the isolable cobalt imidos noted above is only rarely observed, the advent of a library of Co^{II}(Por) complexes that give rise to Co^{III}−nitrenoid radicals [(Por)Co^{III}−$^•$NR] or [(Por$^•$)Co^{III}−($^•$NR)$_2$] has provided numerous instances of highly effective catalytic systems for the stereo-, chemo-, and site-selective aziridination of alkenes and amination of C−H bonds.[19] Starting with Co(TPP), and electron-deficient analogues, several generations of Co^{II}(Por) reagents with richly decorated porphyrins have been introduced in the past two decades to facilitate the activation of various organic azides, leading to the generation of well characterized low-spin (S = 1/2) Co^{III}−$^•$NR moieties, with spin density largely localized on the N atom.[19f,39] These relatively long-lived Co^{III}−nitrene-radical intermediates owe their stability to hydrogen-bonding interactions of the nitrene moieties with porphyrin-appended amido residues (−NHCOR*), which can further introduce and metal-orient chiral auxiliaries via their R* functionality in D_2-symmetric overall geometries. Detailed theoretical and experimental studies[19f,39] have established that the mode of operation of [(Por)Co^{III}−$^•$NR] metalloradicals vis-à-vis C=C or C−H bonds consists of a two-step process: initial formation of a new N−C bond with alkenes and relocation of the spin density on the distal carbon atom (Co^{III}−N(R)−C−$^•$C−) (or formation of a Co^{III}−NHR amido and a substrate-bound radical via hydrogen-atom abstraction from a C−H bond), followed by an essentially barrierless collapse of the carbon-centered radical with the N atom to generate the product of aziridination (or amination) along with Co^{II}(Por).

More recently, the structurally related $[Co^{III}(TAML^{red})]^-$ and $[Co^{III}(TAML^{sq})]$ compounds, featuring the tetraamido macrocyclic ligand TAML in its intact reduced form $TAML^{red}$ and one-electron oxidized variant $TAML^{sq}$ (sometimes denoted as $TAML^{+•}$), have been shown to give rise to $[Co^{III}(TAML^{q})(^•NR)_2]^-$ (S = 1) and $[Co^{III}(TAML^{q})(^•NR)]$ (S = 1/2), respectively ($TAML^{q}$ = doubly oxidized, diamagnetic ligand; Co^{III} site is low-spin, S = 0).[40] These cobalt nitrenes have emerged as capable catalysts for the aziridination of largely styrene substrates by imidoiodinanes (PhINNs, PhINTs, PhINTces).[41] Their mode of operation is considered to be unique, inasmuch as the turnover-limiting, initial N−C bond formation with styrenes features an asynchronous transition state, encompassing a partial electron-transfer to form a styrenyl radical cation, in turn undergoing a *nucleophilic* attack by the

https://doi.org/10.1021/acs.organomet.1c00267
Organometallics 2021, 40, 1974−1996

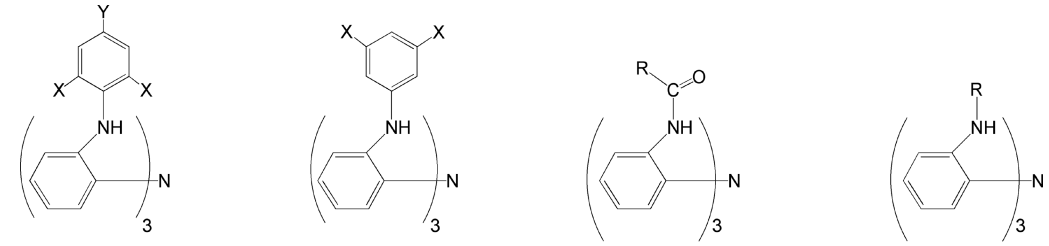

L^1H_3: X = H, Y = *t*-Bu
$L^{11}H_3$: X = Y = Me
$L^{13}H_3$: X = Me, Y = H

L^2H_3: X = *t*-Bu
L^3H_3: X = CF_3
L^5H_3: X = Cl
$L^{12}H_3$: X = Me

L^4H_3: R = *t*-Bu
L^6H_3: R = Ph
L^7H_3: R = *i*-Pr
L^8H_3: R = CF_3
$L^{10}H_3$: R = O*t*Bu
$L^{14}H_3$: R = (*S*)-(−)-CH(Me)(OCOMe)
$L^{15}H_3$: R = C(Ph)(CF_3)(OMe)
$L^{17}H_3$: R = (*S*)-(+)-2,2-Me_2-*c*-C_3H_3

L^9H_3: R = *i*-Pr
$L^{16}H_3$: R = Me

Figure 1. Ligands employed in the present study.

nitrene lone pair (see below for more details). This initial charge-transfer has also emerged as a central component of the operation of iron(IV) imido species developed by Latour and co-workers for alkene aziridinations, further underscoring the importance of the electron affinity of the metal nitrene as a commonly encountered driving force.[42]

Finally, of great interest are recently reported Co(II) organoazides,[43] which either thermally or photolytically can extrude N_2 to give rise to nitrenoids best described as iminyl [Co^{III}−$^{\bullet}$NR] units (R = aryl, alkyl). Although the electronics of these fleeting intermediates are not yet known, crystal structures of such species (R = alkyl) have been determined following N_2 expulsion from single crystals of metal azides in the solid state. For R = aryl, the cobalt(II) organoazide can promote nitrene-transfer by means of unisolable [Co^{III}−$^{\bullet}$NR], both intramolecularly ([3 + 2] annulation) and intermolecularly (C−H allylic amination or styrene aziridination in modest yields). The reactivity of the Co(II) aliphatic azides is more complex and includes (i) α-H atom abstraction via the incipient [Co^{III}−$^{\bullet}$$NCH_2R$] to generate the imine (RCH═NH), if strong δ-C−H bonds (sec, prim) are present; (ii) δ-H atom abstraction and amination of relatively weaker δ-C−H bonds (benzylic, tertiary) by the cobalt alkyl azide itself (initial N_2 extrusion is not needed), leading to substituted pyrrolidines; and (iii) intramolecular 1,3-dipolar cycloaddition of cobalt-bound CH_2═$CH(CH_2)_4N_3$ to afford 1,2,3-dihydrotriazole.

In the present work, we examine a library of high-spin Co(II) reagents (S = 3/2), supported by a modular trisphenylamido-amine ligand framework, giving rise to a weak equatorial field. Previous DFT calculations[44] on one member of this library of reagents indicated that exposure to a nitrene source (PhI = NTs) generates a Co(III)−nitrene radical (Co^{III}−$^{\bullet}$NTs) with a high-spin ground state (S = 5/2). The corresponding doublet and quartet [Co]NTs states lie slightly higher than the sextet by ΔG values of 0.4 and 1.5 kcal mol^{-1}, respectively. The computed spin density for the S = 5/2 state places ∼1.1 unpaired electron on the nitrene N atom, and ∼3.3 unpaired electrons on Co, with the remaining spin density being distributed to other atoms. Similarly to the low-spin porphyrin-supported Co^{III}−nitrene-radical (S = 1/2) noted above, the high-spin congener is capable of performing alkene aziridinations in a two-step process (successive formation of two N−C bonds). Remarkably, the computed transition-state barrier ($\Delta G^{\ddagger}$ = 23.4 kcal mol^{-1} vs Co^{III}−$^{\bullet}$NTs/styrene) for the rate-determining, initial C_{β}···NTs bond-forming step of the high-spin system is very similar to that reported for the corresponding low-spin Co(Por) ($\Delta G^{\ddagger}$ = 24.1 kcal mol^{-1}) or Co(AmidoPor) ($\Delta G^{\ddagger}$ = 22.8 kcal mol^{-1}) with respect to Co^{III}−$^{\bullet}$$NSO_2Ph$/styrene.[19f] The present work significantly enlarges the scope of high-spin Co(II) compounds as nitrene-transfer reagents, and provides insights in their operational characteristics, not only vis-à-vis the reported low-spin (Por)Co(II) paradigms, but also in comparison with the previously examined libraries of Mn(II) and Fe(II) reagents, supported by the same trisphenylamido-amine ligand framework.[44] Whereas the nitrene-transfer reactivity of the Mn(II) reagents in alkene aziridinations largely depends on the electrophilicity of the presumptive Mn^{III}−$^{\bullet}$NR (S = 3/2) moiety, underscoring the role of the electron affinity of the metal nitrene as a dominant factor, the reactivity of the corresponding, more reactive, Co(II) reagents is affected by additional subtle electronic and steric factors. These most likely arise from the tighter disposition of the reaction cavity, resulting in ligand-coordination flexibility, electronic rearrangement, and secondary stabilizing interactions. In this publication we show that even an otherwise small change in ligand substitution can have a significant effect on nitrene-transfer reactivity in aziridination reactions, occasionally overriding the preponderance of the metal-nitrene electrophilicity as a driving force.

RESULTS AND DISCUSSION

Synthesis and Characterization of New Ligands and Co(II) Complexes. The family of trisphenylamido-amine ligands (L^1H_3−$L^{17}H_3$) employed in this study is shown in Figure 1. The majority of these ligands (L^1H_3−$L^{15}H_3$) have been used and reported in previous studies.[44−48] They are all derivatives of the common 2,2′,2″-triaminotriphenylamine framework,[45] featuring carbonaceous arm substituents (alkyl, aryl acyl). Ligand $L^{16}H_3$ is prepared by methylation of deprotonated (KH) 2,2′,2″-triaminotriphenylamine by MeI in THF, and ligand $L^{17}H_3$ is derived via condensation of the same triamine with the corresponding chiral acyl chloride in the presence of Et_3N in dichloromethane. The solid-state structures of these two new ligands (Figure S1) are indicative of their favorable preorganization for metalation, in a cavity that is buttressed by alkyl and acyl arms, respectively.

Co^{II} complexes were synthesized with all ligands, by reacting the deprotonated (KH) ligand with anhydrous beads of $CoCl_2$ in THF (alkyl and aryl armed ligands) or *N*,*N*-dimethylaceta-

https://doi.org/10.1021/acs.organomet.1c00267
Organometallics 2021, 40, 1974−1996

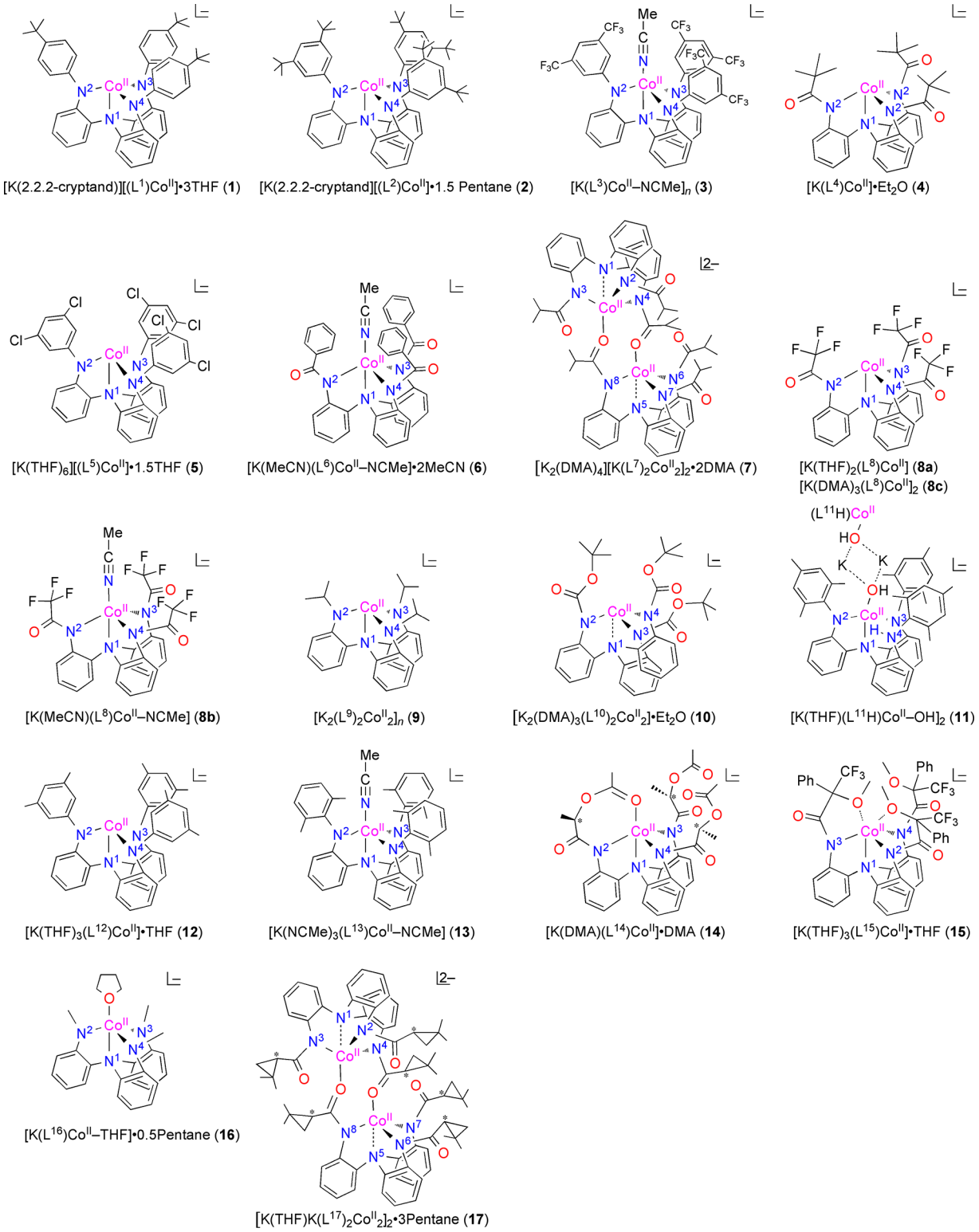

Figure 2. Minimal coordination of Co^{II} compounds with ligands L^1–L^{17} explored in this study.

mide (DMA) (acyl armed ligands). A subset of Co^{II} compounds, namely L^3Co (**3**), L^5Co (**5**), L^8Co (**8a**), L^9Co (**9**), $L^{10}Co$ (**10**), and $L^{13}Co$ (**13**), has been previously reported in a study that examined the use of these catalysts in controlled radical polymerization of olefins.[48] In addition, L^8Co (**8b**) has been explored in conjunction with the L^8 Mn and L^8Fe congeners, toward establishing metal-dependent trends in catalytic nitrene transfer to olefins.[44] Figure 2 depicts representations of the minimal coordination site of each Co^{II} site, derived from single-crystal X-ray diffraction data. In all cases the ligand coordinates in a trigonal pyramidal $[N_{3(amido)}N_{amine}]$ mode, exhibiting various degrees of distortion, although in two instances (**7**, **17**) the coordination to the axial N_{amine} residue can be best described as a long contact. Moreover, compound **11** features a noncoordinating amido residue that has been protonated. The dominant four-coordinate $[N_3N]$ pattern is retained as the sole

https://doi.org/10.1021/acs.organomet.1c00267
Organometallics 2021, 40, 1974−1996

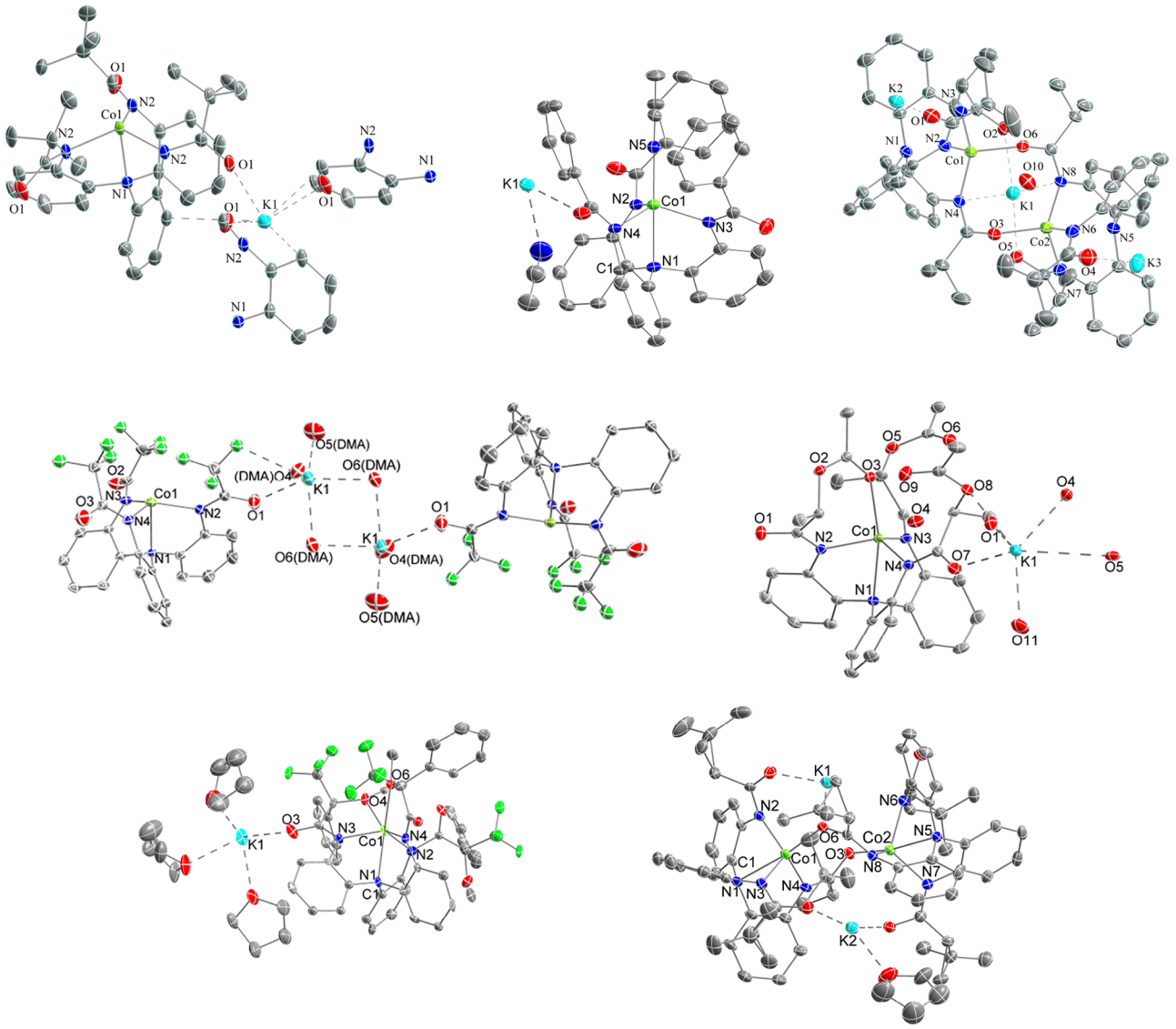

Figure 3. ORTEP diagrams (from left to right) of {[K(L^4)Co^{II}]·Diethyl Ether}$_n$ (**4**), [K(MeCN)(L^6)Co^{II}–NCMe]·2MeCN (**6**), [K_2(DMA)$_4$]-[[K(L^7)$_2Co^{II}_2$]$_2$·2DMA (**7**), [K_2(DMA)$_3$(L^8)Co^{II}]$_2$ (**8c**), [K(DMA)(L^{14})Co^{II}]·DMA (**14**), [K(THF)$_3$(L^{15})Co^{II}]·THF (**15**), and [K(THF)K-(L^{17})$_2Co^{II}_2$]$_2$·3Pentane (**17**), drawn with 40% thermal ellipsoids. Hydrogen atoms are omitted for clarity. Selective interatomic distances (Å) and angles (deg): **4**, Co(1)–N(1) = 2.151(11), Co(1)–N(2) = 1.986(6), Co(1)–[N(2), N(2), N(2)] = 0.32(2) (distance of Co from mean plane) Å, N(2)–Co(1)–N(2) = 117.48(11), N(2)–Co(1)–N(1) = 80.8(2); **6**, Co(1)–N(1) = 2.235(3), Co(1)–N(2) = 2.046(4), Co(1)–N(3) = 2.049(4), Co(1)–N(4) = 2.053(4), Co(1)–N(5) = 2.063(4), Co(1)–[N(2), N(3), N(4)] = 0.48(2) (distance of Co from mean plane), N(2)–Co(1)–N(4) = 115.18(15), N(2)–Co(1)–N(3) = 117.17(15), N(3)–Co(1)–N(4) = 111.69(15), N(2)–Co(1)–N(1) = 76.70(14), N(4)–Co(1)–N(1) = 76.49(14), N(3)–Co(1)–N(1) = 76.15(14), N(3)–Co(1)–N(5) = 103.24(15), N(2)–Co(1)–N(5) = 104.55(14), N(4)–Co(1)–N(5) = 102.81(15), N(1)–Co(1)–N(5) = 178.75(14); **7**, Co(1)–N(1) = 2.463(4), Co(1)–N(2) = 2.053(4), Co(1)–N(3) = 2.054(5), Co(1)–N(4) = 2.054(4), Co(1)–O(6) = 1.975(4), Co(1)–[N(2), N(3), N(4)] = 0.61(2) (distance of Co from mean plane), Co(2)–N(5) = 2.517(5), Co(2)–N(6) = 2.081(5), Co(2)–N(7) = 2.033(5), Co(2)–N(8) = 2.069(5), Co(2)–O(3) = 1.984(4), Co(2)–[N(6), N(7), N(8)] = 0.67(2) (distance of Co from mean plane), N(2)–Co(1)–N(4) = 109.51(18), N(2)–Co(1)–N(3) = 113.66(17), N(3)–Co(1)–N(4) = 111.52(18), N(2)–Co(1)–N(1) = 73.14(16), N(4)–Co(1)–N(1) = 73.24(16), N(3)–Co(1)–N(1) = 71.83(16), N(3)–Co(1)–O(6) = 103.19(17), N(2)–Co(1)–O(6) = 106.85(17), N(4)–Co(1)–O(6) = 111.92(16), N(1)–Co(1)–O(6) = 174.16(15), N(6)–Co(2)–N(7) = 111.14(19), N(6)–Co(2)–N(8) = 112.01(19), N(7)–Co(2)–N(8) = 106.34(19), N(6)–Co(2)–N(5) = 70.48(19), N(7)–Co(2)–N(5) = 70.69(16), N(8)–Co(2)–N(5) = 71.42(17), N(6)–Co(2)–O(3) = 105.77(19), N(7)–Co(2)–O(3) = 105.15(18), N(8)–Co(2)–O(3) = 116.27(17), N(5)–Co(2)–O(3) = 172.25(16); **8c**, Co(1)–N(1) = 2.1422(13), Co(1)–N(2) = 1.9941(14), Co(1)–N(3) = 1.9899(14), Co(1)–N(4) = 1.9872(13), Co(1)–[N(2), N(3), N(4)] = 0.306(4) (distance of Co from mean plane), K(1)–O(1) = 2.7298(14), N(2)–Co(1)–N(4) = 114.79(6), N(2)–Co(1)–N(3) = 118.04(6), N(3)–Co(1)–N(4) = 120.18(6), N(2)–Co(1)–N(1) = 80.83(5), N(4)–Co(1)–N(1) = 81.54(5), N(3)–Co(1)–N(1) = 81.06(5); **14**, Co(1)–N(1) = 2.224(3), Co(1)–N(2) = 2.018(4), Co(1)–N(3) = 2.031(4), Co(1)–N(4) = 2.021(4), Co(1)–O(3) = 2.162(3), Co(1)–[N(2), N(3), N(4)] = 0.42(1) (distance of Co from mean plane), N(2)–Co(1)–N(4) = 110.16(14), N(2)–Co(1)–N(3) = 121.11(15), N(3)–Co(1)–N(4) = 115.82(15), N(2)–Co(1)–N(1) = 76.31(14), N(4)–Co(1)–N(1) = 78.82(13), N(3)–Co(1)–N(1) = 78.58(14), N(3)–Co(1)–O(3) = 106.07(14), N(2)–Co(1)–O(3) = 91.35(13), N(4)–Co(1)–O(3) = 108.68(13), N(1)–Co(1)–O(3) = 167.33(12); **15**, Co(1)–N(1) = 2.337(17), Co(1)–N(2) = 2.041(17), Co(1)–N(3) = 2.048(18), Co(1)–N(4) = 2.033(17), Co(1)–O(4) = 2.405(13), Co(1)–O(6) = 2.302(14), Co(1)–[N(2), N(3), N(4)] = 0.53(2) (distance of Co from mean plane), N(2)–Co(1)–N(4) = 103.6(7), N(2)–Co(1)–N(3) = 118.1(7), N(3)–Co(1)–N(4) = 117.9(7), N(2)–Co(1)–N(1) = 74.3(6), N(4)–Co(1)–N(1) = 76.4(7), N(3)–Co(1)–N(1) = 73.5(6), N(3)–Co(1)–O(6) =

https://doi.org/10.1021/acs.organomet.1c00267
Organometallics 2021, 40, 1974–1996

Figure 3. continued

107.6(6), N(2)−Co(1)−O(6) = 127.7(6), N(4)−Co(1)−O(6) = 73.7(6), N(1)−Co(1)−O(6) = 146.4(6), N(3)−Co(1)−O(4) = 72.9(6), N(2)−Co(1)−O(4) = 89.5(6), N(4)−Co(1)−O(4) = 154.0(6), N(1)−Co(1)−O(4) = 129.3(6), O(4)−Co(1)−O(6) = 80.5(5); **17**, Co(1)−N(1) = 2.428(5), Co(1)−N(2) = 2.055(5), Co(1)−N(3) = 2.038(5), Co(1)−N(4) = 2.047(5), Co(1)−O(6) = 1.990(4), Co(1)−[N(2), N(3), N(4)] = 0.58(1) (distance of Co from mean plane), Co(2)−N(5) = 2.375(5), Co(2)−N(6) = 2.049(5), Co(2)−N(7) = 2.026(5), Co(2)−N(8) = 2.100(5), Co(2)−O(3) = 2.027(4), Co(2)−[N(6), N(7), N(8)] = 0.56(1) (distance of Co from mean plane), N(2)−Co(1)−N(4) = 110.2(2), N(2)−Co(1)−N(3) = 118.9(2), N(3)−Co(1)−N(4) = 107.2(2), N(2)−Co(1)−N(1) = 73.94(18), N(4)−Co(1)−N(1) = 74.25(18), N(3)−Co(1)−N(1) = 72.09(18), N(3)−Co(1)−O(6) = 109.47(18), N(2)−Co(1)−O(6) = 99.64(18), N(4)−Co(1)−O(6) = 110.20(18), N(1)−Co(1)−O(6) = 172.96(17), N(6)−Co(2)−N(7) = 112.3(2), N(6)−Co(2)−N(8) = 113.4(2), N(7)−Co(2)−N(8) = 112.71(19), N(6)−Co(2)−N(5) = 74.71(18), N(7)−Co(2)−N(5) = 74.52(19), N(8)−Co(2)−N(5) = 73.18(17), N(6)−Co(2)−O(3) = 97.07(18), N(7)−Co(2)−O(3) = 112.18(19), N(8)−Co(2)−O(3) = 108.06(17), N(5)−Co(2)−O(3) = 171.18(17).

ligand field of seven Co^{II} compounds (**4**, **5**, **8a**, **8c**, **9**, **10**, **12**). Additional elements of metal coordination, essentially located trans to the axial N_{amine} residue, are observed with all other compounds, and include solvent moieties, especially for compounds crystallized from MeCN (**3**, **6**, **13**) and THF (**16**), as well as carbonyl units (−C(R)═O−Co^{II}) deriving from acyl residues belonging to the ligand (**7**, **14**, **17**). In a single case (**15**), a six-coordinate Co^{II} site arises from the presence of two ligand-derived ether residues in the metal coordination sphere, in addition to the usual [N_3N] framework. Importantly, most structures are polymeric, largely due to an intricate network of intermolecular interactions generated by K^+ ions. Mononuclear (**1**, **2**, **5**, **12**, **13**) or oligonuclear (**8c**, **11**, **17**) compounds (molecular or ionic) are only encountered in a handful of cases. A more detailed description of the structural features of the new Co^{II} compounds is provided below.

Co^{II} Compounds with Acyl-Armed Ligands. The seven new compounds (**4**, **6**, **7**, **8c**, **14**, **15**, **17**; Figure 3) that belong in this category are polymeric, with the exception of [K(DMA)$_3$(L^8)Co^{II}]$_2$ (**8c**) and [K_2(THF)$_2$$K_2$($L^{17}$)$_4$$Co^{II}_4$] (**17**) that feature a dimeric and tetrameric molecular unit, respectively. The catalytically important {[K(L^4)Co^{II}]·Diethyl Ether}$_n$ (**4**) exhibits higher symmetry than all other compounds, consisting of a rigorous 3-fold axis along the Co−N_{amine} direction as well as through K^+ ions relating three different molecules in the crystal lattice. This compound is characterized by an exclusive four-coordinate [N_3N] ligand field and an open metalated cavity fortified by the three −CO^{t}Bu arms. The carbonyl residues are positioned *exo* with respect to the cavity and are further engaged in contacts with K^+ ions, inasmuch as each potassium is coordinated by three oxygen (carbonyl) atoms belonging to different molecules, and is also involved in K^+−arene π contacts. These structural features are largely retained in the structure of [K(NCMe)(L^6)Co^{II}−NCMe]·2MeCN (**6**), but important deviations also apply, mostly because of the presence of a coordinated MeCN molecule in a trans position versus the N_{amine} (N_{amine}−Co−N_{MeCN} = 178.75(14)°) and the lack of a strict 3-fold crystallographic symmetry. Otherwise, each K^+ ion is still coordinated by three carbonyl residues belonging to different molecules in addition to a single MeCN, in lieu of any K^+−arene contacts.

The structure of [K_2(DMA)$_4$][K(L^7)$_2$$Co^{II}_2$]$_2$·2DMA (**7**) is organized in a much more complex manner, featuring a "one-dimensional" array of a repeating unit, [Co(1)/Co(2)−K(1)−Co(3)/Co(4)−K(2)]$_n$, connected to identical arrays via lateral links provided by a DMA solvated K(3)/K(4) dimer (K_2(DMA)$_4$). Within the repeating unit, the Co(II) sites are arranged in two similar dimers linked via K^+ contacts. The dimeric unit is composed of two slightly different Co(II) centers, each featuring the usual [N_3N] ligand coordination, but with a long axial Co−N_{amine} interaction (av. 2.49 Å). In addition, each Co(II) is coordinated by an oxygen atom (carbonyl) positioned *trans* with respect to the axial Co−N_{amine} direction (av. N_{amine}−Co−$O_{C=O}$ = 173.2°, Co−$O_{C=O}$ = 1.98 Å). Importantly, the oxygen atom (carbonyl) coordinated to each Co^{II} center belongs to the ligand surrounding the partner Co^{II} site, hence giving rise to a dimer. The K^+ ions interconnecting the dimers in a pseudo 1-D array are coordinated by two carbonyl and, more weakly, two N_{amido} residues all belonging to one dimer, and by only a single carbonyl moiety (O(10)) belonging to the adjacent dimer. A much more simplified version of this structure is adopted by [K(DMA)$_3$(L^8)Co^{II}]$_2$ (**8c**), exhibiting a dimeric structure comprised of two inversion symmetry related [N_3N]Co^{II} units connected via carbonyl O atoms of acyl residues to a central K_2(μ-DMA)$_2$(DMA)$_4$ core.

Compound [K(DMA)(L^{14})Co^{II}]·DMA (**14**) retains the usual [N_3N] trigonal-pyramidal coordination but exhibits an additional unique feature, inasmuch as one of the chiral arms generates a seven-member loop by positioning the ester carbonyl in the coordination sphere of Co^{II}, trans to the axial N_{amine} residue (N_{amine}−Co−$O_{C=O}$ = 167.33(12)°, Co−$O_{C=O}$ = 2.162(3) Å). The polymeric nature of the compound arises again due to identical K^+ ions, coordinated by one DMA, forming contacts with oxygen residues (amidato carbonyls, MeC(═O)O−) belonging to three different Co^{II} sites in the crystal lattice. Compound [K(THF)$_3$(L^{15})Co^{II}]·THF (**15**) is the only six-coordinate species observed, inasmuch as two acyl arms generate five-membered loops that place two ether residues (ROMe) in the coordination sphere of the [N_3N]Co^{II} site (Co−O = 2.302(14), 2.405(13) Å; N_{amine}−Co−O = 146.4(6), 129.3(6)°). Identical K^+ ions are coordinated by three THF molecules and two acyl residues, each located in neighboring molecules, thus giving rise to pseudo 1-D polymeric structures.

Finally, the structure of [K_2(THF)$_2$][K(L^{17})$_2$$Co^{II}_2$]$_2$ (**17**) is very similar to that observed for **7** with respect to the formation of two interconnecting dimers, but the K^+ ions are organized differently, to afford a molecular (tetranuclear) rather than a polymeric complex. First, two K^+ ions link the two dimers in **17**, by employing the same contact pattern noted for the single K^+ ion connecting the two dimers in **7**. Second, the remaining two K^+ ions in **17** are terminated by THF molecules, and thus do not provide connections that could generate an 1-D array of repeating tetranuclear units as in **7**. Otherwise, the coordination and arrangement of the Co^{II} sites in **17** and **7** is very similar, with somewhat more pronounced contact for the N_{amine} residue (av. Co−N_{amine} = 2.40 Å), and concomitant weaker attachment of the oxygen (carbonyl) moiety (av. Co−$O_{C=O}$ = 2.00 Å), along the axial coordination of Co^{II} sites in **17** versus that of **7**.

https://doi.org/10.1021/acs.organomet.1c00267
Organometallics 2021, 40, 1974−1996

Co^{II} Compounds with Alkyl-Armed Ligands. The new methyl-substituted compound **16** and the previously reported isopropyl congener (**9**)[48] are the only members of the alkyl-armed category of Co(II) compounds explored in this study. Compound **16** (Figure 4) demonstrates the familiar [N_3N]

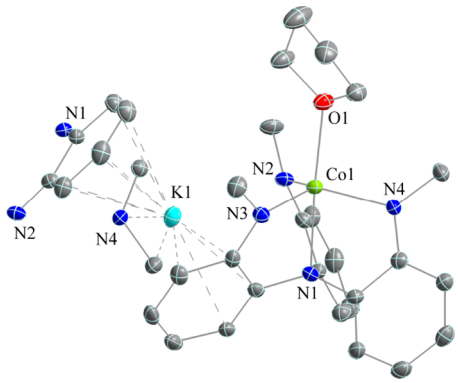

Figure 4. ORTEP diagram of [K(L^{16})Co^{II}−THF]·0.5Pentane (**16**) drawn with 40% thermal ellipsoids. Hydrogen atoms are omitted for clarity. Selective interatomic distances (Å) and angles (deg): Co(1)−N(1) = 2.226(3), Co(1)−N(2) = 2.007(4), Co(1)−N(3) = 1.990(4), Co(1)−N(4) = 2.004(4), Co(1)−O(1) = 2.207(3), Co(1)−[N(2), N(3), N(4)] = 0.37(2) (distance of Co from mean plane), N(2)−Co(1)−N(4) = 112.70(15), N(2)−Co(1)−N(3) = 114.04(15), N(3)−Co(1)−N(4) = 122.94(15), N(2)−Co(1)−N(1) = 79.40(13), N(4)−Co(1)−N(1) = 78.61(14), N(3)−Co(1)−N(1) = 79.64(14), N(3)−Co(1)−O(1) = 100.45(14), N(2)−Co(1)−O(1) = 104.32(13), N(4)−Co(1)−O(1) = 97.91(14), N(1)−Co(1)−O(1) = 175.75(13).

coordination, but unlike the more bulky isopropyl analogue, it exhibits a five-coordinate Co^{II} site due to the presence of a coordinated THF molecule trans to the N_{amine} residue (N_{amine}−Co−O_{THF} = 175.75(13)°). The electron-rich alkyl substitution dictates a stronger equatorial ligand field (av. Co−N_{amido} = 2.000 Å) by comparison to all other five-coordinate Co^{II} sites investigated in this study. The polymeric nature of the compound arises by means of a repeating −[Co(1)−K(1)]− sequence, which features K(1) ions engaging in K−N_{amido} and K^+−arene contacts with both ligands of adjacent Co(1) sites.

Co^{II} Compounds with Aryl-Armed Ligands. Among the seven aryl-supported Co(II) reagents shown in Figure 2 (**1**, **2**, **11**, **12** are new; **3**, **5**, **13** have been previously reported[48]), only those crystallized from MeCN solutions (**3**, **13**) feature a solvent molecule coordinated to the Co(II) center. All others, crystallized from THF solutions, exhibit four-coordinate [N_3N]Co(II) sites devoid of any axial THF residues, in sharp contrast to analogous five-coordinate Mn and Fe reagents previously reported.

Among the four new Co(II) complexes (Figure 5), (L^1)Co (**1**) provides nice green crystals from concentrated THF solutions, but single-crystal specimens (albeit of low quality) were only obtained in the presence of the exceptional K^+ binder 2.2.2-cryptand. The resulting ionic complex [K(2.2.2-cryptand)][(L^1)Co^{II}]·3THF (**1**) exhibits a distorted [N_3N] coordination with an equatorial ligand field (av. Co−N = 1.927 Å) that is equal or stronger than that demonstrated by similar four-coordinate Co(II) sites supported by aryl substituents (**2**, **5**, **12**), presumably due to the electron-rich character of the 4-^{t}Bu-substituted phenyl arm. Similarly, the 3,5-^{t}Bu_2 disubstituted compound (L^2)Co (**2**) proved to be isolable only in the presence of 2.2.2-cryptand, in the form of green crystals of [K(2.2.2-cryptand)][(L^2)Co^{II}]·1.5Pentane (**2**) of marginal quality. Its structure is almost identical with that of **1**, with a similarly strong equatorial field (av. Co−N = 1.927 Å). The corresponding 3,5-Me_2 disubstituted compound [K-$(THF)_3$(L^{12})Co^{II}]·THF (**12**) is monomeric and geometrically analogous to **2**, with a weaker equatorial field (av. Co−N = 1.956 Å), but, as opposed to **1** and **2**, can be isolated without the assistance of 2.2.2-cryptand. The K^+ ion in **12** is supported by three THF molecules and a host of contacts with aromatic moieties and N atom residues.

Although both the 3,5-Me_2 and 2,6-Me_2 disubstituted compounds **12** and **13**, respectively, can be isolated and characterized, the corresponding 2,4,6-Me_3 trisubstituted species (L^{11})Co^{II} has proven to be difficult to synthesize, apparently due to extreme sensitivity to even traces of water. In contrast, the analogous [$K(THF)_3$(L^{11})Mn^{II}−THF] can be readily prepared.[44] Indeed, after initial formation of a deep green species in the reaction of deprotonated $L^{11}H_3$ and $CoCl_2$ in THF, the color soon fades and ligand can be recovered intact along with separation of blue $Co(OH)_2$. In one instance, under scrupulous water exclusion, a few green crystals of [K(THF)-(L^{11}H)Co^{II}−OH)]$_2$ (**11**) have been isolated, amounting to a species that can be viewed as the formal product of water addition to (L^{11})Co^{II}. Indeed, **11** features protonation and dissociation of one nitrogen residue from the equatorial field, with concomitant formation of a Co^{II}−OH moiety. The hydroxide is further coordinated by two K(THF)$^+$ ions in an overall dimeric structure that connects two inversion-related (L^{11}H)Co^{II}−OH monomers by means of a $K_2(OH)_2$ rhomb.

Structures Featuring Ligand Rearrangement. In two instances, we have isolated a few compounds that exhibit a characteristic oxidative ligand rearrangement in the presence of traces of dioxygen or one-electron oxidants. Similarly reorganized compounds, featuring electron-donor substituents, have been previously studied in our lab and attributed to the formation of an incipient aminyl radical.[45b,49] Indeed, the electron-rich (L^2)Co^{II} (**2**) is highly sensitive to oxidative rearrangement, and provided two crystallographically characterized species, [$K(THF)_3$(L^2_{re})Co^{II}−THF] (**2b**) and [($L^2_{re,ox}$)-Co^{II}−THF]·0.5 Pentane (**2c**) (Scheme 1 and Figure S2; bonds broken in **2** and formed in **2b** and **2c** are shown in red), formed in comparable amounts. Compound **2c** is not only ligand-rearranged, but also one-electron oxidized, as noted by relevant metrical parameters associated with the phenylene ring between atoms N_1 and N_2 (Figure S2). A possible overall stoichiometry for this reaction can be written as 2[(L^2)Co^{II}]$^-$ → [(L^2_{re})Co^{II}]$^-$ + [($L^2_{re,ox}$)Co^{II}] + e^-.

Compound (L^{16})Co^{II} (**16**) is also highly sensitive to the same type of ligand rearrangement in the presence of traces of dioxygen, affording the isolable dimer [$K(THF)_2$(L^{16}_{re})Co^{II}]$_2$ (**16b**, Figure S3), which is equivalent to **2b** in terms of ligand reorganization. In this case, we were not able to isolate any other compound that might provide evidence for the location of the oxidizing equivalent(s).

Electrochemistry. Ten Co(II) compounds possessing aryl (L^3Co, L^5Co, L^{13}Co), alkyl (L^9Co), and acyl arms (L^4Co, L^6Co, L^7Co, L^8Co, L^{10}Co, L^{17}Co) were selected as representative examples for examination by cyclic voltammetry. Electrochemical data for a handful of these examples have been previously reported.[48] Figure 6 provides a collective presentation of the corresponding waves (first oxidation event), and Table S2 summarizes relevant electrochemical data (potentials

https://doi.org/10.1021/acs.organomet.1c00267
Organometallics 2021, 40, 1974−1996

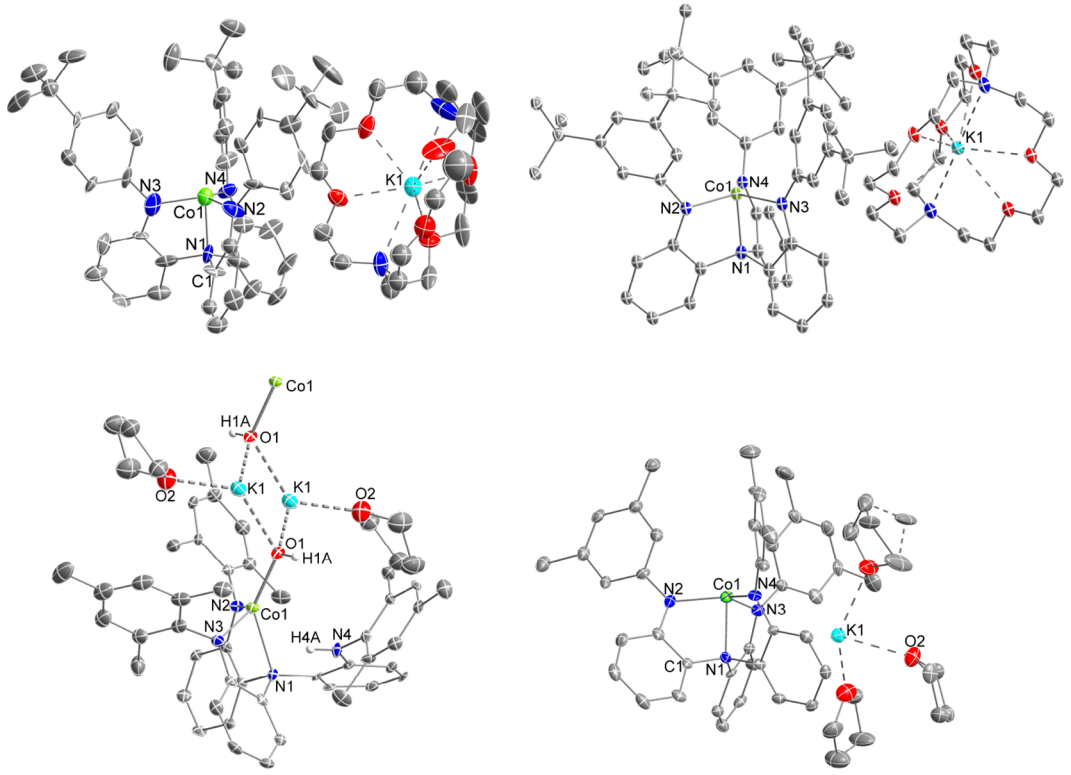

Figure 5. ORTEP diagrams (from left to right) of [K(2.2.2-cryptand)][(L^1)Co^{II}]·3THF (**1**), [K(2.2.2-cryptand)][(L^2)Co^{II}]·1.5Pentane (**2**), [K(THF)(L^{11}H)Co^{II}−OH]$_2$ (**11**), and [K(THF)$_3$(L^{12})Co^{II}]·THF (**12**) drawn with 40% thermal ellipsoids. Hydrogen atoms are omitted for clarity. Selective interatomic distances (Å) and angles (deg): **1**, Co(1)−N(1) = 2.102(18), Co(1)−N(2) = 1.946(18), Co(1)−N(3) = 1.92(2), Co(1)−N(4) = 1.915(19), Co(1)−[N(2), N(3), N(4)] = 0.17(2) (distance of Co from mean plane), N(2)−Co(1)−N(4) = 122.7(8), N(2)−Co(1)−N(3) = 118.0(8), N(3)−Co(1)−N(4) = 117.0(8), N(2)−Co(1)−N(1) = 84.0(8), N(4)−Co(1)−N(1) = 85.1(8), N(3)−Co(1)−N(1) = 85.6(8); **2**, Co(1)−N(1) = 2.085(8), Co(1)−N(2) = 1.921(7), Co(1)−N(3) = 1.933(8), Co(1)−N(4) = 1.926(7), Co(1)−[N(2), N(3), N(4)] = 0.14(1) (distance of Co from mean plane), N(2)−Co(1)−N(4) = 120.4(3), N(2)−Co(1)−N(3) = 118.2(3), N(3)−Co(1)−N(4) = 119.8(3), N(2)−Co(1)−N(1) = 85.9(3), N(4)−Co(1)−N(1) = 86.0(3), N(3)−Co(1)−N(1) = 85.5(3); **11**, Co(1)−N(1) = 2.260(5), Co(1)−N(2) = 1.956(5), Co(1)−N(3) = 1.939(5), Co(1)−O(1) = 1.947(4), K(1)−O(1) = 2.675(5), K(1)−O(2) = 2.677(5), Co(1)−[N(2), N(3), N(4)] = 0.62(2) (distance of Co from mean plane), N(2)−Co(1)−N(3) = 118.7(2), N(2)−Co(1)−N(1) = 81.6(2), N(3)−Co(1)−N(1) = 80.1(2), N(1)−Co(1)−O(1) = 139.41(18), N(2)−Co(1)−O(1) = 108.5(2), N(3)−Co(1)−O(1) = 122.9(2), Co(1)−O(1)−K(1) = 113.83(18), O(1)−K(1)−O(2) = 116.95(15); **12**, Co(1)−N(1) = 2.121(7), Co(1)−N(2) = 1.950(8), Co(1)−N(3) = 1.964(8), Co(1)−N(4) = 1.955(7), Co(1)−[N(2), N(3), N(4)] = 0.20(1) (distance of Co from mean plane), N(2)−Co(1)−N(4) = 119.2(3), N(2)−Co(1)−N(3) = 121.5(3), N(3)−Co(1)−N(4) = 116.2(3), N(2)−Co(1)−N(1) = 84.3(3), N(4)−Co(1)−N(1) = 84.0(2), N(3)−Co(1)−N(1) = 84.0(3).

Scheme 1

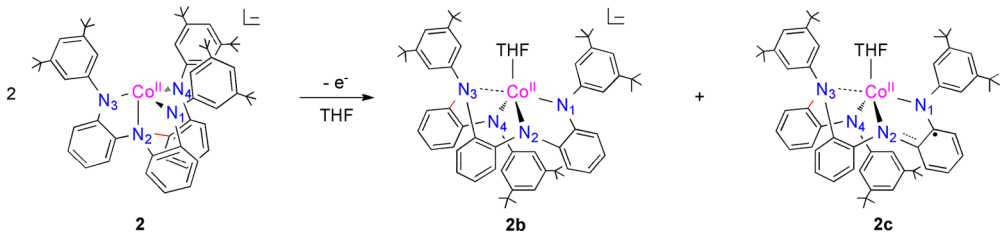

are reported versus the ferrocenium/ferrocene (F_c^+/F_c) couple). All aryl- and alkyl-armed Co(II) compounds examined by cyclic voltammetry feature semireversible waves at negative potentials, ranging from −0.665 (L^{13}Co) to −0.090 V (L^3Co), in accordance with the electron-rich nature of the corresponding substituents. Specifically for the alkyl-armed L^9Co, the two closely spaced, semireversible waves observed (−0.654, −0.500 V), may represent the two slightly different Co(II) sites in the crystal structure. Given the almost identical wave currents for all these aryl- and alkyl-armed Co(II) compounds (3.0 M), and their anodic shifts with respect to the analogous Mn(II)/Mn(III) and Fe(II)/Fe(III) couples[44,46a] by approximately 0.65 and 0.25 V, respectively, we assign the corresponding semireversible waves to essentially metal-centered Co(II)/Co(III) cycles.

In sharp contrast, the acyl-armed Co(II) compounds examined demonstrate irreversible anodic ways with variable $i_{p,a}$ values (mostly large versus the aryl/alkyl-substituted congeners), suggesting significant ligand-centered contributions. In addition, the first anodic wave shown in Figure 6 overlaps with a subsequent oxidation wave (not shown), rendering any attempts to garner further information from exhaustive electrolysis futile. Nevertheless, all initial anodic waves for the acyl-armed Co(II) sites are shifted to positive

https://doi.org/10.1021/acs.organomet.1c00267
Organometallics 2021, 40, 1974−1996

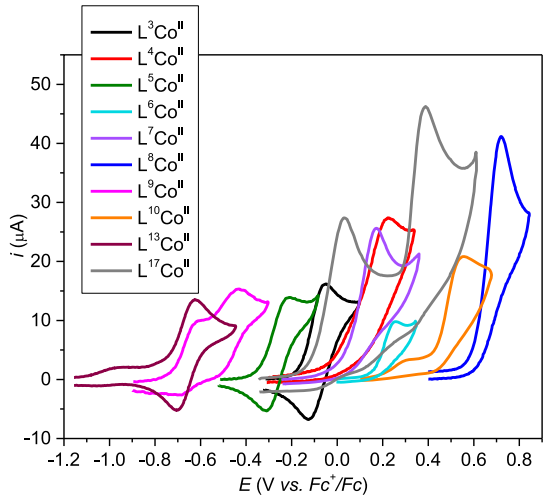

Figure 6. Cyclic voltammograms of compounds $[K(L^3)Co^{II}{-}NCMe]$ (**3**) and $[K(NCMe)_3(L^{13})Co^{II}{-}NCMe]$ (**13**) in MeCN/$(^nBu_4N)PF_6$, $[K(L^4)Co^{II}]\cdot Et_2O$ (**4**), $[K(THF)_6][(L^5)Co^{II}]\cdot 1.5THF$ (**5**), $[K(MeCN)(L^6)Co^{II}{-}NCMe]\cdot 2MeCN$ (**6**), $[K_2(DMA)_4][K(L^7)_2Co^{II}{}_2]_2\cdot 2DMA$ (**7**), $[K(THF)_2(L^8)Co^{II}]$ (**8a**), $[K_2(L^9)_2Co^{II}{}_2]$ (**9**), and $[K(THF)K(L^{17})_2Co^{II}{}_2]_2\cdot 3Pentane$ (**17**) in DMF/$(^nBu_4N)PF_6$, and $[K_2(DMA)_3(L^{10})_2Co^{II}{}_2]\cdot 0.5Et_2O$ (**10**) in DMA/$(^nBu_4N)PF_6$, with a Au disk electrode (1.6 mm in diameter); scan rate 0.1 V/s.

potentials (0.032 (L^{17}Co) to 0.719 V (L^8Co)), reflecting the effect of the electron-withdrawing acyl arm on the Co(II) center, albeit in an order not always consistent with the electronic nature of each individual acyl group. The most significant deviation is observed for L^{10}Co ($E_{p,a}$ = 0.559 V), whose anodic shift versus that of L^{10} Mn ($E_{p,a}$ = −0.108 V; tentatively assigned to Mn(II)/Mn(III))[44] betrays very little, if any, metal-centered contributions to the anodic wave. The intervention of ligand-centered oxidation events does not permit any secure identification of the solution structure of species such as L^7Co and L^{10}Co, which exhibit single anodic waves even in the presence of dinuclear units in their polymeric solid-state structures. On the other hand, the dual anodic-wave feature for L^{17}Co (solid-state tetramer) may signify a dinuclear structure in solution. Finally, the catalytically important L^8Co ($-COCF_3$ arm) possesses the indisputably most electrochemically stable Co(II) site encountered in this series of Co(II) compounds, in agreement with previous findings for the L^8 Mn and L^8Fe analogues.[44,46a]

EPR Spectroscopy. EPR spectra of selected Co(II) compounds were recorded from frozen DMF solutions of **3**, **4**, **5**, **6**, 7, **8a**, **9**, **10**, **13**, **14**, **15**, and **17**. In all cases, the samples give rise to signals that are consistent with isolated Co^{II} (S = 3/2) species.[50] Spectra recorded at 10 K are shown in Figure 7. The spectra can be interpreted within the framework of the spin Hamiltonian:[51]

$$\hat{H}_{zfs} = D\left[\hat{S}_z^2 - \frac{S(S+1)}{3} + \frac{E}{D}(\hat{S}_x^2 - \hat{S}_y^2)\right] + \hat{\mathbf{S}}\cdot\mathbf{A}\cdot\hat{\mathbf{I}} + \beta\mathbf{B}\cdot\mathbf{g_0}\cdot\hat{\mathbf{S}} \quad (1)$$

In eq 1, D and E are the zero field splitting (zfs) parameters. **A** is the hyperfine tensor relevant to the hyperfine interactions of the electronic (S = 3/2) and nuclear (I = 7/2 for ^{59}Co) spins, and $\mathbf{g}_0$ is the intrinsic **g**-tensor of the Co(II) ion. For simplicity we assume that the principle axes of the tensors are parallel to each other. Often, due to large spin orbit coupling effects for Co^{II} (S = 3/2), the zfs parameter $|D|$ is quite large, whereas **A** and $\mathbf{g}_0$ are characterized by significant anisotropy. Under the influence of zfs, the 4-fold degeneracy is partially lifted in zero magnetic field, yielding two Kramers' doublets, $|\pm 1/2\rangle$ and $|\pm 3/2\rangle$ separated by $2|D|$. The $|\pm 1/2\rangle$ (or $|\pm 3/2\rangle$) doublet is the ground

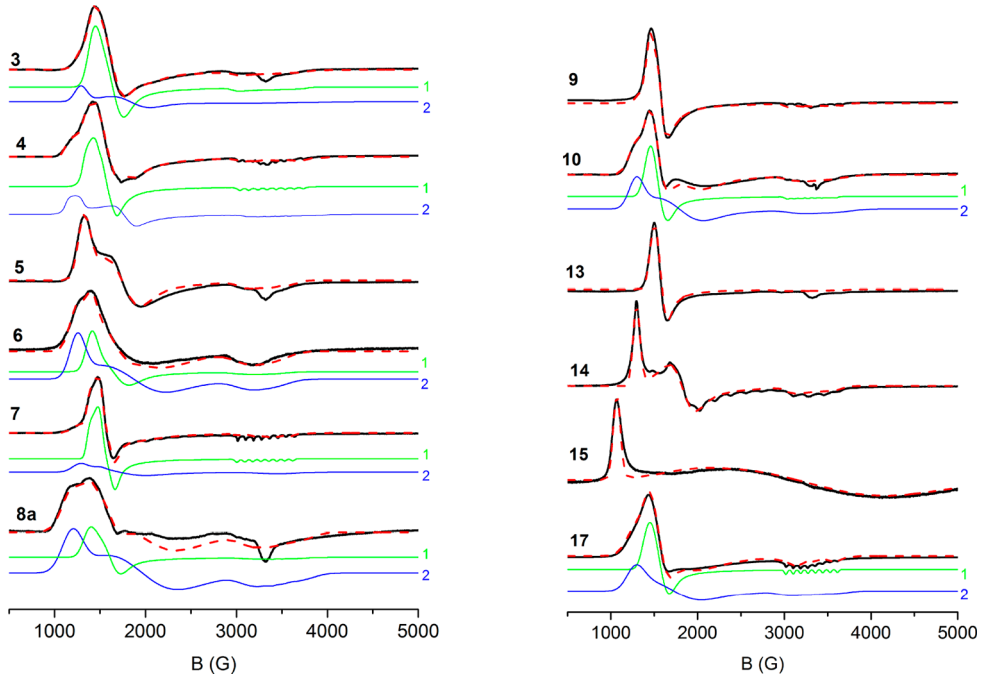

Figure 7. Experimental (black line) and theoretical (red-dashed line) EPR spectra from frozen DMF solutions of complexes **3**, **4**, **5**, **6**, 7, **8a**, **9**, **10**, **13**, **14**, **15**, and **17**. For **3**, **4**, **6**, 7, **8a**, **10**, and **17**, the subspectra from sites 1 (green), and 2 (blue) are also shown, as described in the text. A spike signal at ca. 3400 G in the spectra of **5**, **9**, and **10** is due to an impurity in the cavity. EPR conditions: Temperature, 10 K; modulated amplitude 10 Gpp; microwave power, 2.0 mW; microwave frequency, 9.4 GHz.

https://doi.org/10.1021/acs.organomet.1c00267
Organometallics 2021, 40, 1974−1996

state for positive (or negative) D. For $|D| \gg h\nu$ (≈ 0.31 cm^{-1} at X-band), each Kramers' doublet can be described by an effective $S_{eff} = 1/2$, giving rise to an EPR spectrum characterized by an anisotropic $\mathbf{g}_{eff}$ tensor.

The EPR signals shown in Figure 7 are consistent with the $|\pm 1/2\rangle$ doublet. No detailed temperature dependence of the spectra was pursued in the present work. However, spectra recorded at 4.2 and/or 20 K (not shown) indicate that the intensity of the signals (scaled as Intensity × Temperature) decreases as temperature increases. This suggests that the $|\pm 1/2\rangle$ doublet is the ground state, implying a positive value for D. For $|D| \gg h\nu$, the spectra observed do not depend on D but rather on the rhombic zfs parameter E/D, the values of the intrinsic $\mathbf{g}_0$-tensor,[52] and the hyperfine term. With the exception of the spectrum for complex **15**, the $\mathbf{g}_0$-tensor was assumed axial ($\mathbf{g}_{0x} = \mathbf{g}_{0y} = \mathbf{g}_{0\perp} \neq \mathbf{g}_{0z} = \mathbf{g}_{\parallel}$). In several cases (**3**, **4**, **6**, **7**, **8a**, **10**, **17**), the spectra indicated the presence of two Co(II) species, characterized by a different value for the parameter E/D. Assuming a common value for $|D|$, the simulations determine the relative abundance of each Co(II) site. The specific line shape of the spectra results from a combination of factors, including distributions on the parameter E/D (E/D strain), unresolved hyperfine interactions, and residual line-broadening mechanisms.[53] The EPR parameters for all samples, as well as the relative ratios of the two species when applicable, are presented in Table S3. Because an unequivocal deconvolution of the line broadening mechanisms is not feasible, the quoted values for the relevant parameters are indicative.

With the exception of the six-coordinate **15**, all other complexes (four- or five-coordinate) exhibit rhombic parameters (E/D) that lie in the interval [0, 0.19], indicating different degrees of rhombicity. All complexes (except **15**) demonstrate a valley-shaped signal at $\mathbf{g} \sim 2.0$, which corresponds to the $\mathbf{g}_{\parallel}$ component of the $\mathbf{g}_{eff}$-tensor. This signal is broadened due to hyperfine interactions, and in some cases (**7**, **9**, **17**) the hyperfine lines are well resolved. The simulations indicate that $\mathbf{A}_{\parallel}$ values in all cases are in the range of 200−300 MHz and that the hyperfine term has to be taken into account in order to reproduce the low field region of the spectra, corresponding to the perpendicular components of the tensors in eq 1. Due to restrictions in the determination of the line-broadening mechanisms, it is not possible to unambiguously evaluate the magnitudes of the $\mathbf{A}_x$ and $\mathbf{A}_y$. Therefore, an average value, $\mathbf{A}_{\perp} = (\mathbf{A}_x + \mathbf{A}_y)/2$, is quoted in Table S3. This value ranges in the 30−90 MHz range. Complex **15** exhibits a relatively sharp peak at $g = 6.24$ and an extremely broad derivative feature with an apparent zero crossing at ca. $g = 2.07$. This behavior indicates a rhombic system with $E/D = 0.33$. From this point of view, complex **15** exhibits unique EPR properties in this series, most likely due to its special, six-coordinate ligand field, featuring two O residues in addition to the familiar $[N_3N]$ coordination. The origin of dual EPR-active species in DMF solutions of some compounds cannot be ascertained at the present time, especially since structural data from crystals derived from DMF solutions are not available. Possible sources are small deviations in the coordination of Co(II) sites in polymeric species (as noted for **7**, crystallized from DMA solutions), and also potential differentiation arising from partial DMF coordination to Co(II) and even K^+ sites.

In summary, the EPR studies from frozen DMF solutions of the complexes indicate that all complexes feature a Co(II) ($S = 3/2$) ion with a large and positive zfs term, D, and variable degree of rhombicity. The existence of more than one species in some cases suggest that the coordination environment of the Co ion can be quite flexible in solution.

Catalytic Aziridinations of Olefins. *Styrene.* The 17 Co^{II} compounds shown in Figure 2 were first explored as catalysts (5 mol %) for the aziridination of styrene (8.0 equiv) by PhINTs (1.0 equiv) in chlorobenzene at room temperature (Table 1).

Table 1. Yields of Styrene Aziridination Mediated by Co^{II} Reagents 1−17[a]

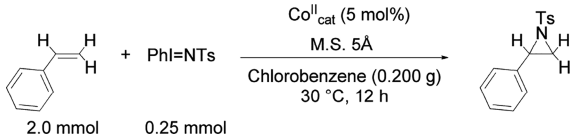

compound	yield (%)
$[K(2.2.2\text{-cryptand})][(L^1)Co^{II}]\cdot 3THF$ (**1**)	18
$[K(2.2.2\text{-cryptand})][(L^2)Co^{II}]\cdot 1.5Pentane$ (**2**)	18
$[K(L^3)Co^{II}{-}NCMe]$ (**3**)	36
$[K(L^4)Co^{II}]\cdot Diethyl\ Ether$ (**4**)	**70**
$[K(THF)_6](L^5)Co^{II}]\cdot 1.5THF$ (**5**)	32
$[K(NCMe)(L^6)Co^{II}{-}NCMe]\cdot MeCN\cdot 0.5H_2O$ (**6**)	50
$[K_2(DMA)_4][K(L^7)_2Co^{II}{}_2]_2\cdot 2DMA$ (**7**)	59
$[K(NCMe)(L^8)Co^{II}{-}NCMe]$ (**8b**)	69
$[K(DMA)_3(L^8)Co^{II}]_2$ (**8c**)	68
$[K_2(L^9)_2Co^{II}{}_2]_n$ (**9**)	38
$[K_2(DMA)_3(L^{10})_2Co^{II}{}_2]\cdot 0.5Et_2O$ (**10**)	49
$[K(THF)(L^{11}H)Co^{II}{-}OH)]_2$ (**11**)	–
$[K(THF)_3(L^{12})Co^{II}]\cdot THF$ (**12**)	25
$[K(NCMe)_3(L^{13})Co^{II}{-}NCMe]$ (**13**)	38
$[K(DMA)(L^{14})Co^{II}]\cdot DMA$ (**14**)	36
$[K(THF)_3(L^{15})Co^{II}]\cdot THF$ (**15**)	45
$[K(L^{16})Co^{II}{-}THF]$ (**16**)	25
$[K(THF)K(L^{17})_2Co^{II}{}_2]_2$ (**17**)	35

[a]Conditions: Catalyst, 0.0125 mmol (5 mol %); PhINTs, 0.25 mmol; styrene, 2.0 mmol; MS 5 Å, 20 mg; PhCl, 0.200 g; 30 °C; 12 h.

The high-yielding L^4Co^{II} was first investigated as catalyst in several solvents (MeCN, 50%; 2,2,2-Trifluoroethanol, 62%; $PhCF_3$, 61%; CH_2Cl_2, 61%; Benzene, 53%; PhCl, 70%) and found to afford superior levels of aziridine in chlorobenzene (similar solvent-screening results were previously obtained with Mn^{II} reagents[44]). The yield drops significantly (25%) if equimolar amounts of styrene and PhINTs are employed in PhCl, whereas a 2-fold excess of styrene over PhINTs improves the yield to 46%. Increasing the amount of the L^4Co catalyst to 10 mol % suppresses the yield to 53%. The styrene aziridination yields obtained with various Co^{II} catalysts (Table 1) vary significantly (18−70%) as a function of the ligand employed. As opposed to the corresponding L^xMn^{II} reagents ($x = 1$−15)[44] that reveal a dominant relationship between increasing styrene aziridination yields with anodically shifting Mn^{II}/Mn^{III} redox potentials (and, by extension, with increasing electrophilicity of the putative $Mn^{III}{-}^{\bullet}NR$), the Co^{II} catalysts provide yields that indicate a more complex pattern of electronic and steric contributions. For example, although the comparatively electron-deficient, acyl-armed reagents remain, on average, more productive than aryl- or alkyl-armed congeners, a comparison between the $-COCMe_3$ (L^4) and $-COCF_3$ (L^8) supported Co^{II} reagents furnishes essentially the same aziridination yields, in spite of the fact that the Co(II)/Co(III) couple for L^8Co is anodically shifted by ∼500 mV versus L^4Co. In addition, L^8Co is potentially less congested than L^4Co. In

https://doi.org/10.1021/acs.organomet.1c00267
Organometallics 2021, 40, 1974−1996

Table 2. Yields of Aziridination/Amination of Olefins by $[K(L^4)Co^{II}]\cdot Et_2O$ (4)[a]

Entry No.	Substrate	Products		Yield (%) CH_2Cl_2/PhCl L^4Co
1.	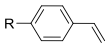	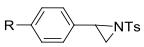	R = H	61/70
2.			R = Me	52/70
3.			R = ^{t}Bu	55/72
4.			R = OMe	30/40
5.			R = O^{t}Bu	33/72
6.			R = F	31[b]/56/71
7.			R = Cl	45[b]/52/71
8.			R = CF_3	36/49
9.			R = NO_2	36/39
10.	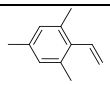	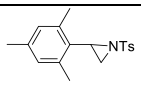		39
11.		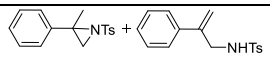		59, 3
12.		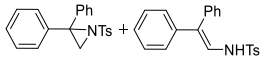		5, 15
13.	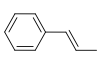	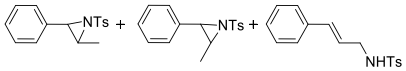		41, nd, 1
14.		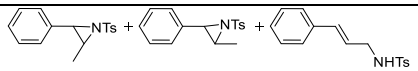		21, 31, tr
15.		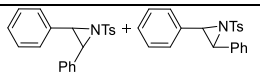		6, 8
16.	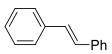	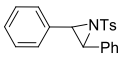		7
17.	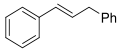	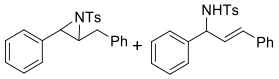		24, 21
18.		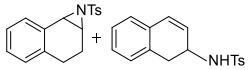		27, nd
19.		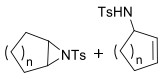	n = 1	9, 12
20.			n = 2	7, 10
21.			n = 4	41, nd
22.		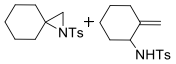		19, 20

[a]Conditions: **4**, 0.0125 mmol (5 mol %); PhINTs, 0.25 mmol; olefin, 2.0 mmol; MS 5 Å, 20 mg; solvent (MeCN/CH_2Cl_2/PhCl) 0.200 g; 30 °C; 12 h. [b]In MeCN.

contrast, the Mn^{II} and Fe^{II} congeners are associated with significantly diverging yields in favor of the more electron-deficient L^8M reagents (L^4Mn, 12%; L^8Mn, 75%; L^4Fe, 45%; L^8Fe, 73%), correlating with an anodic potential shift of approximately 600 mV for both the L^8Mn and L^8Fe catalysts with respect to their L^4M analogues. More importantly, as indicated below, L^4Co (**4**) is faster than L^8Co (**8b**, **8c**) in mediating styrene aziridination. The closely related L^7Co (−CO^{i}Pr arm) is in principle slightly less electron rich and sterically congested than the L^4Co congener, but affords lower yields than L^4Co in a slower reaction (the opposite is true for the corresponding Mn(II) catalysts).[44] Two other acyl-substituted Co^{II} catalysts ($L^{14}Co$, $L^{17}Co$), exhibiting significantly lower yields, are indicative of how the metal-nitrene electron-affinity bias may be overridden by other electronic or steric factors in the fairly restricted reaction cavity of Co reagents. The corresponding L^{14} Mn catalyst, by contrast, is among the most productive Mn^{II} aziridination reagents examined (yield: 67%).[44] As expected, the aryl-substituted ligands generate Co^{II} reagents that are poor mediators of styrene aziridination. These sites are oxidatively and even hydrolytically sensitive and tend to generate thermodynamic sinks. Nevertheless, the muted role of the electron-affinity criterion can still be discerned in the series of the electron-rich, aryl-armed reagents (**1**, **2**, **3**, **5**, **12**, **13**), inasmuch as the highest-yielding $L^{13}Co$ (**13**) is the most electron rich member of the group. Finally, the alkyl-substituted L^9Co and $L^{16}Co$ reagents are only modestly productive, as anticipated for electron-rich Co^{II} sites, but again the more

https://doi.org/10.1021/acs.organomet.1c00267
Organometallics 2021, 40, 1974−1996

electron rich, isopropyl-substituted L^9Co provides higher yields than the methyl-substituted congener $L^{16}Co$. However, the latter undergoes facile oxidative ligand rearrangement that may compromise its structural integrity.

*Alkene Aziridinations by [K(L^4)Co^{II}]·Diethyl Ether (**4**).* The highest yielding L^4Co (**4**) catalyst was subsequently investigated as a nitrene-transfer (NTs) mediator with a panel of aromatic, cyclo (Table 2), and aliphatic alkenes (Table S4). Styrenes substituted at the *para* position with both electron-donor and electron-acceptor groups were examined first (entries 1−9) under the conditions noted in the previous section. Both methylene chloride and chlorobenzene were employed (as well as acetonitrile in a few instances), invariably resulting in better aziridination yields in chlorobenzene. In the majority of cases, yields above 70% were recorded irrespective of the electron-rich or poor character of the substituent, with the exception of two moderately yielding cases involving strong electron-withdrawing groups (*p*-CF_3, *p*-NO_2). Moreover, the product of 4-MeO-styrene aziridination is known to be unstable,[54] and is thus associated with modest yields. Overall, the aziridination yields for these *para*-substituted styrenes, save for the parent styrene, are comparable to those previously reported for L^8Co. *Ortho*-substitution (entry 10) affects aziridination yields, presumably interfering with nitrene-transfer both sterically and electronically (due to the orthogonal orientation of the aromatic versus the olefinic plane of the substrate[55]). Similar steric inhibition is also observed for α-substituted styrenes (methyl, phenyl; entries 11 and 12), especially for the bulkier α-phenyl-styrene. An allylic amination product is also obtained in both cases, ascribed to aziridine-ring opening,[56] which is more pronounced for the α-phenyl-substituted product.[54] Steric hindrance is also evident in the aziridination of β-substituted styrenes (entries 13−16), especially for the bulky *cis*- and *trans*-stilbene (entries 15, 16). In agreement with previous observations in the application of L^8Co,[44] the cis congeners are more productive (entries 14, 15), with significant loss of stereochemical integrity. For all these encumbered substrates, L^8Co is on average more productive than L^4Co, presumably reflecting the somewhat more voluminous reaction cavity of L^8Co. Allylic or benzylic aminations compete successfully with aziridinations (entries 17−22), unless cis (entry 18) and/or electron-rich (entry 21) olefins are involved. Beyond cycloalkenes, other terminal or internal aliphatic olefins exhibit low aziridination yields (Table S4), in accordance with previous results pertaining to the application of L^8Co in aziridinations of aromatic and aliphatic olefins.[44] A competitive styrene versus 1-hexene (1.0 mmol each) aziridination by PhINTs (0.25 mmol) catalyzed by L^4Co (5 mol %) in chlorobenzene provided a ratio of 25:1 in favor of the styrene aziridination product (combined aziridine yield: 72%), not unlike the L^8Co catalyst (28:1, yield 73%).[44]

Mechanistic Studies. *Comparative Reaction Profile.* The formation of the product of styrene aziridination was monitored as a function of time (Figure 8) for catalysts L^4Co (**4**), L^7Co (**7**), and L^8Co (**8c**) (all crystallized from DMA/ether), under the conditions noted above (Table 1), with the exception of the amount of PhCl used (500 mg). Yields were determined after quenching the reaction at various time intervals. Surprisingly, the more electron rich and sterically congested L^4Co (**4**) exhibits faster product generation than L^8Co (**8c**) during the first hour, whereas L^7Co (**7**) is kinetically comparable to **8c**. At the 1.0 h mark, the reaction is complete by 88% for L^4Co (**4**), 65% for L^8Co (**8c**), and 76% for L^7Co (**7**). Interestingly, the MeCN-crystallized version of L^8Co, [K(NCMe)(L^8)Co^{II}−NCMe] (**8b**), has been previously shown[44] to be significantly slower; only 14% of the reaction is complete after 1.0 h in d^5-PhCl, indicating potential interference by the strongly coordinating acetonitrile. However, **8b** is still much faster than the corresponding [K(NCMe)(L^8)M^{II}−NCMe] (M = Mn, Fe) reagents, presumably reflecting the superior electrophilicity of Co^{III}−•NR as discerned from $E_{p,a}$ values associated with the M^{II}/M^{III} couple of the divalent catalysts (Fe: 0.228 V, Mn: 0.518 V, Co: 0.837 V).[44]

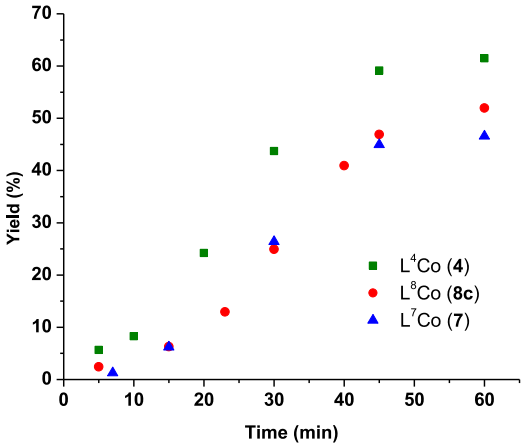

Figure 8. Yield of aziridine (%) as a function of time (min) in the reaction of styrene (2.0 mmol) by PhI = NTs (0.25 mmol) mediated by L^4Co (**4**), L^8Co (**8c**), and L^7Co (**7**) (0.0125 mmol with respect to Co) in chlorobenzene (0.500 g) at 30 °C.

Hammett Analysis. Several *para*-substituted styrenes (*para* substituent: Me, ^{t}Bu, F, Cl, CF_3, NO_2; 1.0 mmol each) were subjected to competitive aziridination (PhINTs, 0.25 mmol) versus styrene (1.0 mmol), mediated by L^4Co (5 mol %) in chlorobenzene (0.200 g), in the presence of 5 Å molecular sieves (25 mg). Hammett plots of $\log(k_X/k_H)$ (determined by ^{1}H NMR from the ratio of the corresponding aziridines) as a function of the substituent polar parameter σ_P or even the resonance-responsive parameter σ^+ did not provide any reliable linear free-energy correlations (Figure S4, Table S5). In contrast, Jiang's dual-parameter correlation that incorporates both polar (σ_{mb}) and spin-responsive (σ_{JJ}*) parameters ($\log(k_X/k_H) = \rho_{mb}\sigma_{mb} + \rho_{JJ}*\sigma_{JJ}* + C$)[57] provides a reasonable linear correlation (R^2 = 0.98; Figure 9). The negative ρ_{mb} value is

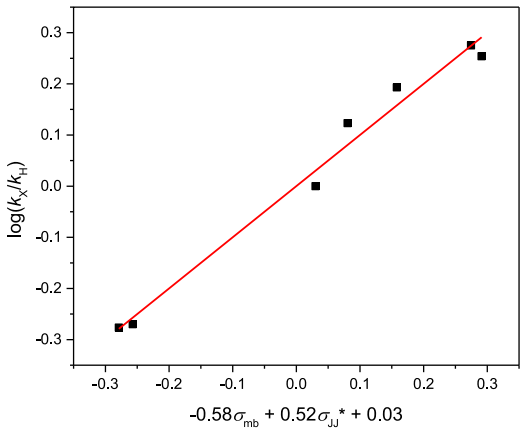

Figure 9. Linear free energy correlation of $\log(k_X/k_H)$ vs σ_{mb}, σ_{JJ}* for the aziridination of *para*-substituted styrenes (X = Me, ^{t}Bu, F, Cl, CF_3, NO_2) mediated by L^4Co (**4**).

https://doi.org/10.1021/acs.organomet.1c00267
Organometallics 2021, 40, 1974−1996

consistent with a small positive charge developing at the benzylic carbon, whereas the always positive ρ_{JJ}* value denotes an incipient radical character for the same site. The ratio $|\rho_{mb}/\rho_{JJ}^*|$ = 1.12 is similar to the one previously observed for L^8Co catalyzed aziridinations ($|\rho_{mb}/\rho_{JJ}^*|$ = 1.0),[44] and indicates competitive contributions of polar and spin-delocalization effects. Polar effects are dominant in many Rh,[24d] Cu,[24d,58] and Fe[18g,59,60] catalyzed aziridinations, for which Hammett plots can be fit with the assistance of polar parameters alone (σ_p, σ^+), but the need for incorporating spin-delocalization parameters (σ^*, σ_{JJ}^*)[57,61] with a wide range of $|\rho_{mb}/\rho_{JJ}^*|$ values (0.04−2.02) is also evident in many other metal-catalyzed aziridinations.[18e,22d,g,23f,g] More recently, larger $|\rho^+/\rho_{JJ}^*|$ values have been reported for the aziridination of styrene by PhINNs mediated by $[Co^{III}(TAML^{red})]^-$ (5.71) and $[Co^{III}(TAML^{sq})]$ (8.64), in accordance with a novel mechanism that involves a partial single-electron transfer from the styrene to the metal-nitrene as a component of the turnover-determining step.[41] A similar mechanistic scenario has also been advanced for Fe-mediated aziridinations, but in this case Hammett correlations can be successfully accommodated with polar parameters alone (σ^+).[42]

Kinetic Isotope Effect and Stereochemical Integrity. Evaluation of the secondary kinetic isotope effect was accomplished by ^{1}H and ^{2}H NMR with the assistance of deuterated styrenes (*α-d*-styrene, *cis-* and *trans-β-d*-styrene; 1.0 mmol each) in competitive aziridinations (PhINTs, 0.25 mmol) with styrene (1.0 mmol) catalyzed by L^4Co (**4**) or L^8Co (**8c**) (5 mol %) in chlorobenzene (Table 3). KIE values close to 1.0 were

Table 3. Secondary KIE Values in Aziridination of Deuterated Styrenes vs Styrene

Catalyst			
$[K(L^4)Co^{II}]_n$ (**4**)	1.01(±0.01)	0.90(±0.02)	0.92(±0.02)
$[K(DMA)_3(L^8)Co^{II}]_2$ (**8c**)	1.00(±0.01)	0.96(±0.02)	0.98(±0.02)

obtained with *α-d*-styrene for both catalysts, indicating that the *α*-styrenyl is unlikely to be involved in the initial nitrene attack to styrene. In contrast, the *β*-styrenes are associated with inverse KIE values for L^4Co (cis: 0.90 (±0.02), trans: 0.92 (±0.02)) that can be attributed to a limited $sp^2 \rightarrow sp^3$ rehybridization of styrene's C_β site upon development of the initial N−C_β bond (Scheme 2). More modest inverse KIE values are also noted in *cis-* and *trans-β-d*-styrene aziridinations mediated by L^8Co (**8b**[44] or **8c**) (cis: 0.96 (±0.02), trans: 0.98 (±0.02)), suggesting only minimal N−C_β bond formation in the transition state.

The kinetics of the aziridine ring closure (formation of the second N−C_α bond) was further evaluated by ^{2}H NMR in the aziridinations of *cis-* and *trans-β-d*-styrene (Table 4), by examining the degree of stereochemical scrambling in the resulting aziridines (cis/trans partitioning due to C_α−C_β bond rotation; Scheme 2) in competition with N−C_α bond formation. The ratio of cis/trans aziridine (94:6) and trans/cis aziridine (92:8) resulting from the L^4Co-mediated aziridination of *cis-β-d*-styrene and *trans-β-d*-styrene, respectively, signifies the interference of very small energy barriers in aziridine-ring closure. A slightly larger barrier is indicated for the aziridination of the more sensitive *cis-β-d*-styrene by L^8Co (cis/trans aziridine: 89/11). On the other hand, the stereochemical scrambling observed in the aziridination of *cis-β*-methyl-styrene is more pronounced with L^4Co than L^8Co.

Computational Studies. The structure and electronic description of the presumptive $[L^4Co]$NTs intermediate were explored by DFT calculations at the B3LYP/6-31+G(d) level of theory. Free energy calculations suggest that the intermediate-spin quartet ground state (S = 3/2) lies only 0.1 kcal mol^{-1} lower than the high-spin sextet state (S = 5/2), and 2.8 kcal mol^{-1} below the doublet state (S = 1/2). As mentioned above, the calculated free energies for $[L^8Co]$NTs indicate that the high-spin sextet is the ground state, in agreement with the weaker ligand field provided by the L^8 versus L^4 ligand.

Calculated structures for the three spin-states of $[L^4Co]$NTs along with key metrical parameters are presented in Figure 10. The most conspicuous feature of these structures is the dissociation of one arm from the equatorial coordination sphere of the metal (Co−N = 3.93 (quartet), 3.67 (sextet), 4.08 (doublet) Å). The axial Co−N_{amine} bond is also elongated (Co−N = 2.43 (quartet), 2.63 (sextet), 2.99 (doublet) Å), if not dissociated, by comparison to that of L^4Co (2.151(11) Å). These features have been previously noted in the DFT structure of $[L^8Co]$NTs, although the latter exhibits an additional Co−F equatorial contact (Co−F = 2.37 Å).[44]

Most importantly, the calculated spin densities for all three spin states of $[L^4Co]$NTs place a full oxidizing equivalent over the dissociated arm, hence generating a widely delocalized *N*-aryl amidyl radical (Figure 11). For the ground-state quartet, the computed spin density consists of ~3.2 unpaired e$^-$ on Co, 0.79 e$^-$ on the nitrene N atom and −1.0 unpaired e$^-$ on the noncoordinating arm. Similar spin densities are calculated for the sextet (Co: 2.9 e$^-$, N: 0.9 e$^-$, ligand arm: 1.0 e$^-$) and the doublet state (Co: 2.8 e$^-$, N: −0.66 e$^-$, ligand arm: −1.0 e$^-$). This spin density distribution is accommodated by an electronic structure such as $[(^\bullet L^4)Co(II)-^\bullet NTs]^-$, featuring a high-spin Co(II) center (S = 3/2) and two oxidizing equivalents on the noncoordinating ligand arm and the N atom of the nitrene residue, respectively. In sharp contrast, the spin density of the ground-state sextet of $[L^8Co]$NTs (Figure 11) is largely distributed on Co (3.3 e$^-$) and the N atom of the nitrene (1.1 e$^-$). In this case, the noncoordinating arm is redox innocent, and the residual spin density is centered over ligating N atoms in a typical spin polarization fashion. Hence, the sextet state of $[L^8Co]$NTs is better accommodated with an $[(L^8)Co(III)-^\bullet NTs]^-$ electronic description (S_{Co} = 2).

Scheme 2

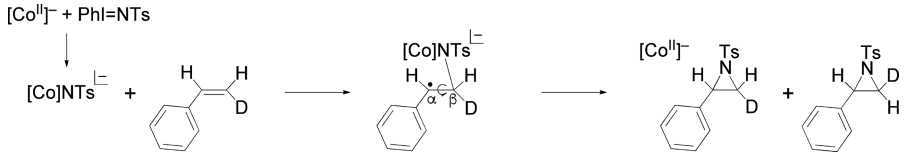

https://doi.org/10.1021/acs.organomet.1c00267
Organometallics 2021, 40, 1974−1996

Table 4. Exploration of Stereochemical Integrity in the Aziridination of *cis*- and *trans*-β-*d*-Styrene

Catalyst	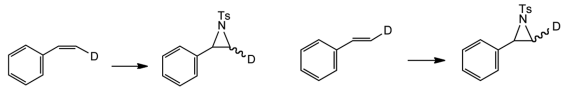	
$[K(L^4)Co^{II}]_n$ (**4**)	94:6 (cis:trans aziridine)	92:8 (trans:cis aziridine)
$[K(DMA)_3(L^8)Co^{II}]_2$(**8c**)	89:11 (cis:trans aziridine)	92:8 (trans:cis aziridine)

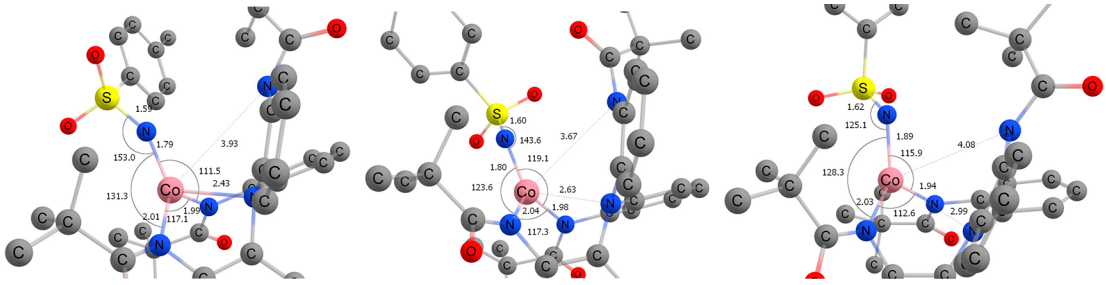

Figure 10. DFT structures (minimal metal coordination) for $[L^4Co]$NTs active species in different spin states (from left to right: quartet, sextet, doublet) optimized at the B3LYP/6-31+G(d) level of theory. Hydrogen atoms were omitted from the figure for clarity.

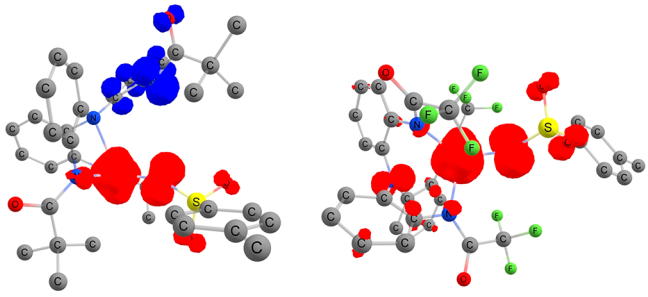

Figure 11. Spin density on the calculated lowest-energy spin state of the putative cobalt nitrenoid intermediates: quartet $[L^4Co]$NTs (left) and sextet $[L^8Co]$NTs (right).

A global electrophilicity index (GEI) was also computed for $[L^4Co]$NTs and $[L^8Co]$NTs by employing Stephan's improved methodology.[62] For the quartet spin state, GEI is calculated to be 5.0 eV for $[L^4Co]$NTs and 5.7 eV for $[L^8Co]$NTs. The corresponding values for the sextet spin state are 4.7 and 6.1 eV for $[L^4Co]$NTs and $[L^8Co]$NTs, respectively. Thus, $[L^8Co]$NTs is more electrophilic than $[L^4Co]$NTs on the basis of the GEI criterion.

Unfortunately, all efforts to map the aziridination reaction coordinate starting from $[L^4Co]$NTs and styrene have not been successful in locating an acceptable transition state for the initial N−C_b bond formation. All three spin states (quartet, sextet, doublet) of $[L^4Co]$NTs generated large activation barriers for this initial step (~50 kcal/mol). However, when dispersion-corrected DFT was applied,[63] as appropriate for polarizable bulky groups such as the *tert*-Bu, the corresponding barriers were reduced by approximately 20 kcal/mol. These barriers are still significant by comparison to those we have previously identified for the reaction of $[L^8Co]$NTs (sextet) and styrene (23.4 kcal/mol for the turnover-limiting N−C_b bond formation).[44] Further experimentation and attendant DFT calculations will be required to unravel reliable trends and contributing factors with the assistance of catalysts that feature substituents spanning the CF_3 to CMe_3 range.

FURTHER DISCUSSION AND CONCLUSIONS

In a rigorous recent account, Latour and co-workers[42] highlight the importance of the electron affinity (EA) of iron-nitrene/imido species as a guiding principle for predicting their reactivity in a wide range of iron-mediated aziridinations. In these catalytic reactions, the iconic substrate styrene undergoes aziridinations by various iron-nitrene compounds (Fe = NR), under a general mechanistic scheme that designates the formation of the initial N−C_b bond as the rate-determining step, usually encountered in aziridinations with a two-step mechanism ([M]NR radical addition to styrene, ring-closure radical rebound). More importantly, this first step is front-loaded by significant charge transfer from styrene to the iron-nitrene and, thus, is crucially influenced by the EA of the active oxidant. The applicability of the EA as a general predictor of reactivity seems to be wide, but at the present time is largely confined within the realm of catalysts that provide Hammett correlations for the aziridination of *para*-substituted styrenes that can be accommodated with polar parameters alone (σ_p, σ^+), or by a combination of polar and spin-delocalization parameters (σ^*, σ_{JJ}^*) with dominant polar contribution.

In an almost concurrent publication, de Bruin and co-workers[41] advance a similar argument with the assistance of electrophilic Co(III)-nitrene radical aziridination reagents, generated from the reaction of anionic $[Co^{III}(TAML^{red})]^-$ or the one-electron oxidized and neutral $[Co^{III}(TAML^{sq})]$ with PhINNs. Hammett plots for *para*-substituted styrene aziridinations are fitted with both polar (σ^+) and spin-delocalization parameters (σ_{JJ}^*) with large $|\rho^+/\rho_{JJ}^*|$ values (5.71 for $[Co^{III}(TAML^{red})]^-$ and 8.64 for $[Co^{III}(TAML^{sq})]$), hence these systems can also be considered as good candidates for testing the EA criterion. Indeed, the larger $|\rho^+/\rho_{JJ}^*|$ value for $[Co^{III}(TAML^{sq})]$ and DFT calculations indicate that the energy barrier for the initial, rate-limiting reaction of the incipient $[Co^{III}]$NNs and styrene to generate the N−C_b bond is lower for $[Co^{III}(TAML^{sq})]$ versus $[Co^{III}(TAML^{red})]^-$, in agreement with an anticipated higher EA value for the nitrene species generated from $[Co^{III}(TAML^{sq})]$. Surprisingly, the experimental rate for

https://doi.org/10.1021/acs.organomet.1c00267
Organometallics 2021, 40, 1974−1996

the aziridination of styrene by these two catalysts favors $[Co^{III}(TAML^{red})]^-$ versus $[Co^{III}(TAML^{sq})]$, but this has been attributed largely to the instability of the latter reagent. A distinctive feature of the Co(III) systems is associated with the redox noninnocent character of the tetraanionic ligand $(TAML^{red})^{4-}$, which can be successively oxidized in one-electron steps to $(TAML^{sq})^{3-}$ and $(TAML^{q})^{2-}$. The authors argue convincingly that the emerging radical nitrene species $[Co^{III}(TAML^{sq})(^{\bullet}NNs)]^-/Co^{III}(TAML^{q})(^{\bullet}NNs)_2]^-$ and $[Co^{III}(TAML^{q})(^{\bullet}NNs)]$, resulting from $[Co^{III}(TAML^{red})]^-$ and $[Co^{III}(TAML^{sq})]$, respectively, interact with styrene in the rate-limiting step by means of an asynchronous transition state, encompassing significant single-electron transfer from styrene to the oxidized TAML ligand and a *nucleophilic* attack by the nitrene lone pair (in lieu of the $^{\bullet}$NNs *p* radical) at the incipient styrenyl radical cation. The attendant single-electron relocation (TAML → Co(III) → $^{\bullet}$NNs) reestablishes the N lone pair and retains the Co(III) oxidation state. Similar participation of charge transfer in the rate-limiting transition state between high-valent metal nitrenes/imidos and sulfides has been recently showcased for many other nitrene-transfer catalysts[64] and is now established as a common mechanistic feature.

In a previous comprehensive study from our lab,[44] we have shown that a library of Mn(II) catalysts, supported by the vast majority of the ligands used in the present work ($L^{1-15}H_3$), mediates alkene aziridinations with reactivity that increases in parallel with increasing electrophilicity of the putative $[Mn^{III}]-^{\bullet}$NTs active oxidant. Moreover, the electrophilicity criterion holds across the base metals, inasmuch as the reactivity of the best performing Mn(II) reagent L^8Mn is inferior to that of the more acidic L^8Co. Although the electron affinity of the metal-nitrene reigns supreme for all these reagents, the molecular interaction between $[M^{III}]-^{\bullet}$NR and styrene in the rate-limiting formation of the initial N−C_b bond, is quite distinct with respect to the reagents explored by Latour and de Bruin. Indeed, Hammett correlations for the aziridination of styrenes mediated by our L^8M reagents (M = Mn, Fe, Co) reveal rather modest positive charge buildup on the α-styrenyl carbon (increasing with metal acidity in the expected order: Fe < Mn < Co), and require the inclusion of competitive spin-delocalization contributions ($|\rho_{mb}/\rho_{JJ}^*|$ = 0.75 (Mn), 1.17 (Fe), 1.00 (Co); the correlation for Fe was rather weak). The fact that these reagents demonstrate more modest charge-transfer characteristics is consistent with the operation of presumptive metal nitrenes ($[M^{III}]-^{\bullet}$NR) resting at a lower oxidizing level than the high-valent iron and cobalt nitrenes of Latour and de Bruin, respectively. Overall, these Mn(II) reagents and congeners can also be accommodated under the general EA criterion advanced by Latour (after all, they are catalysts engaged in typical electrophilic radical reactions), although they are not characterized by a dominant charge-transfer component. Incidentally, a strongly enhanced radical contribution, as in the case of Betley's iron dipyrrinato complexes ($|\rho_{mb}/\rho_{JJ}^*|$ = 0.04 for NAd),[18e] has been interpreted[42] as the result of a competitive energy barrier for the second, ring-closing step (radical rebound).

The library of the Co(II) reagents (S = 3/2) reported in this work showcases some surprising deviations from the EA criterion. Although the importance of the electrophilicity of the metal-nitrene can still be detected in the relative enhanced yields provided by the Co(II) compounds possessing acyl- versus aryl- or alkyl-substituted ligands, the trend is certainly not as smooth and predictable as that previously encountered with the Mn(II) reagents.[44] Indeed, a closer inspection of the acyl-substituted subset of the Co(II) library of reagents reveals a wide range of yields in the aziridination of styrene that cannot be correlated with the anticipated electrophilicities of the corresponding cobalt-nitrene moieties. To further pinpoint the provenance of these disparities, we selected the high-yielding L^8Co (−$COCF_3$ arm) and L^4Co (−$COCMe_3$ arm) for further investigation. The L^8Co was previously studied[44] in tandem with the L^8Mn and L^8Fe congeners and found to be more reactive and selective than the other two base metal analogues. Mechanistic and computational studies showed that all three L^8 M reagents follow a two-step styrene aziridination path (turnover-limiting addition of $[L^8 M^{III}]-^{\bullet}$NTs to the β-styrenyl carbon followed by product-determining ring-closure via radical rebound), with activation barriers in the order Fe > Mn > Co for both steps. The trend is consistent with the anticipated metal-nitrene electrophilicities (first step) and ease of reduction from M(III) to M(II) (second step), hence highlighting the dominant role of EA *in both steps* of styrene aziridination (aliphatic olefins do not follow the same trend for the second step).

The representative case of L^4Co, however, presents a conundrum, inasmuch as its reactivity in terms of styrene aziridination yields is comparable to that provided by L^8Co. More importantly, the rate of product buildup in the first hour of the reaction mediated by L^4Co is superior to that of L^8Co (Figure 8). These results are difficult to reconcile for a reagent such as L^4Co, whose Co(II/III) couple is cathodically shifted by 500 mV versus that of L^8Co, and its nitrene derivative $[L^4Co]$NTs is computed to have a lower global electrophilicity index (GEI) than that of $[L^8Co]$NTs, in agreement with the electronic nature of the CMe_3 and CF_3 substituents. In addition, the enhanced reactivity of L^4Co deviates from that of the corresponding L^4Mn and L^4Fe reagents, which exhibit significantly lower yields (and rates) in styrene aziridinations by comparison to the L^8Mn and L^8Fe analogues, in line with their electrophilic characteristics.

Mechanistic analysis of the operation of L^4Co in styrene aziridination indicate that both polar (σ_{mb}) and spin-delocalization (σ_{JJ}^*) parameters are needed to fit Hammett plots, suggesting that both modest positive charge buildup and radical stabilization participate in the turnover-limiting step. The unexpected preponderance of the polar effect for L^4Co by comparison to L^8Co can be traced both in the slightly higher values of absolute ρ_{mb} (−0.58) and relative $|\rho_{mb}/\rho_{JJ}^*|$ (1.17) than those observed for L^8Co (ρ_{mb} = −0.56, $|\rho_{mb}/\rho_{JJ}^*|$ = 1.0). The secondary KIE values obtained from the competition between styrene and selectively deuterated styrene in aziridinations confirm that both catalysts operate via an initial, turnover-limiting N−C_b bond formation step, but also indicate that the L^4Co mediated pathway incorporates more significant rehybridization of the β-styrenyl carbon in the transition state, hence placing this TS energetically closer to the resulting radical intermediate $[L^4Co]N(Ts)-CH_2-^{\bullet}CH_2Ph$. Moreover, the ring-closing step (radical rebound) seems to operate via a miniscule energy barrier for both L^4Co and L^8Co styrene aziridinations, but the one for L^4Co is even more suppressed than that for L^8Co, as judged by the superior retention of stereochemistry in the aziridination of the sensitive substrate *cis*-β-styrene. This runs counter to what is usually the main driving force for the aziridine-ring closure of styrene, namely the ease of reduction from Co(III) to Co(II).[22g,44,65] All these mechanistic observations would have been perfectly in line, had the supporting L^4 ligand been more electron-withdrawing than L^8.

https://doi.org/10.1021/acs.organomet.1c00267
Organometallics 2021, 40, 1974−1996

DFT calculations on the electronic and geometric disposition of the presumptive [L⁴Co]NTs vis-à-vis the previously explored [L⁸Co]NTs highlight how a small ligand modification can result in a major electronic rearrangement. First, the ground state of [L⁴Co]NTs is computed to be the quartet (S = 3/2), positioned slightly underneath the sextet (S = 5/2). The sextet is the clear ground state of [L⁸Co]NTs, presumably due to the weaker ligand field provided by the L⁸ ligand. Geometrically, both cobalt nitrenes are quite similar, their most outstanding feature being the elongation of one of the equatorial N residues to a noncoordinating position. However, spin-density calculations reveal that the noncoordinating arm of [L⁴Co]NTs is one-electron oxidized, whereas the corresponding arm of [L⁸Co]NTs is redox innocent. The single-electron distribution of the resulting *N*-aryl amidyl radical in [L⁴Co]NTs is spread throughout the noncoordinating arm, with almost half of the spin density being localized on the N atom. Apparently, the electron withdrawing CF_3 residue protects the noncoordinating arm of [L⁸Co]NTs from a similar one-electron oxidation. The overall electronic picture for the ground state of the two cobalt nitrenes is schematically summarized in Figure 12. As noted above, the [L⁴Co]NTs sextet (α-spin on the N-aryl amidyl radical) is calculated to be only 0.1 kcal/mol higher in free energy relative to the quartet.

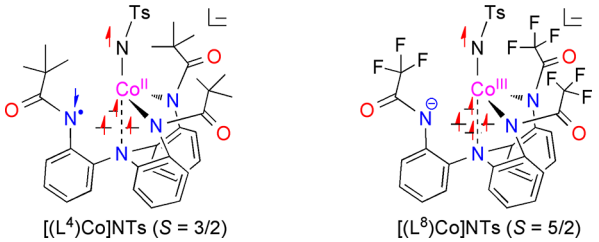

Figure 12. Schematic distribution of spins in the ground state of [L⁴Co]NTs and [L⁸Co]NTs.

Whereas a definitive justification for the higher reactivity of L⁴Co, in spite of lower electrophilicity, versus L⁸Co cannot be provided at the present time, the following observations should be taken into account:

(i) Although it cannot be excluded, it is deemed rather unlikely that the ease of formation of the cobalt-nitrene itself (presumably favoring [L⁴Co]NTs) will be a contributing factor, since our previous calculations for the reaction of [L⁸M^II] (M = Mn, Fe, Co) and PhINTs indicate almost instantaneous generation of [L⁸M]NTs. Rate-limiting metal-nitrene formation is more common with organic azides (RN_3).[66]

(ii) The fact that L⁴M (M = Mn, Fe), as well as a wide range of other Mn(II) reagents, exhibit reactivities consistent with the EA criterion, whereas L⁴Co and other Co(II) reagents demonstrate deviations, suggest that ligand-centered contributions to the overall oxidizing ability of the reagent may enable more favorable reactivity channels. Indeed, [LCo^III]NTs is more likely to store oxidizing equivalents on ligand residues, as inferred by the cyclic voltammograms of the LCo^II reagents, and anticipated due to the superior oxidizing power of Co(III) versus Mn(III) or Fe(III). Among other possibilities, *N*-aryl amidyl radicals are known to add to alkenes, at least intramolecularly,[67] and more electrophilic *N*-aryl sulfonamidyl radicals can even add intermolecularly.[68] Although they are not expected to outcompete the metal-bound nitrene radical, they might offer stabilizing interactions not yet realized. On the other hand, the similarity of the Hammett parameters for L⁴Co and L⁸Co suggests that the electronic differences in the ground states of [L⁴Co]NTs and [L⁸Co]NTs may have only a small effect on their reactivities, but this point requires further elaboration once more information is available for the corresponding transition states.

(iii) Multiple spin-state reactivity channels,[65c,69] such as those offered by the almost isoenergetic quartet and sextet states of [L⁴Co]NTs, may afford enhanced reactivity profiles in aziridinations[70] by comparison to a potentially single spin-state operation by the [L⁸Co]NTs sextet.

(iv) London dispersion (LD) interactions applying intramolecularly between highly polarizable alkyl substituents (also known as $\sigma-\sigma$ interactions) are now well established stabilizing forces of sterically congested molecules in solution, by means of favorable enthalpic contributions.[71] The *tert*-Bu group and other conformationally rigid alkyl groups (flexible alkyl groups have an unfavorable entropic impact)[72] have been credited as "dispersion energy donors",[73] and deemed responsible for stabilizing many highly congested organic and inorganic compounds.[71−74] More importantly, LD forces have started receiving recognition as contributors to observed chemical reactivity and catalytic outcomes.[75] In the more tight reaction cavity of cobalt reagents, the stabilization offered by *tert*-Bu groups via LD interactions can play a significant role, as already noted in our initial dispersion-corrected DFT calculations. Interestingly, the L⁷Co reagent, which carries the less polarizable *i*-Pr substituent, demonstrates lower aziridination rates, not unlike those of L⁸Co.

Future experimental and computational research will seek to disentangle and quantify the factors contributing to the enhancement of catalytic reactivity above and beyond the underlying electrophilic character of the active oxidant, and further explore whether reagents with other rigid alkyl substituents can be superior mediators of nitrene-transfer chemistry.

■ ASSOCIATED CONTENT

Supporting Information

The Supporting Information is available free of charge at https://pubs.acs.org/doi/10.1021/acs.organomet.1c00267.

Experimental procedures; physicochemical characterization of new compounds; crystallographic information; catalytic and mechanistic data (PDF)

Accession Codes

CCDC 2069526−2069535 and 2069537−2069542 contain the supplementary crystallographic data for this paper. These data can be obtained free of charge via www.ccdc.cam.ac.uk/data_request/cif, or by emailing data_request@ccdc.cam.ac.uk, or by contacting The Cambridge Crystallographic Data Centre, 12 Union Road, Cambridge CB2 1EZ, UK; fax: +44 1223 336033.

■ AUTHOR INFORMATION

Corresponding Authors

Thomas R. Cundari − *Department of Chemistry, Center for Advanced Scientific Computing and Modeling (CASCaM), University of North Texas, Denton, Texas 76203, United*

https://doi.org/10.1021/acs.organomet.1c00267
Organometallics 2021, 40, 1974−1996

States; orcid.org/0000-0003-1822-6473; Email: thomas.cundari@unt.edu

Pericles Stavropoulos − *Department of Chemistry, Missouri University of Science and Technology, Rolla, Missouri 65409, United States*; Email: pericles@mst.edu

Authors

Anshika Kalra − *Department of Chemistry, Missouri University of Science and Technology, Rolla, Missouri 65409, United States*

Vivek Bagchi − *Department of Chemistry, Missouri University of Science and Technology, Rolla, Missouri 65409, United States; Institute of Nano Science and Technology, Mohali, Punjab 160062, India*

Patrina Paraskevopoulou − *Inorganic Chemistry Laboratory, Department of Chemistry, National and Kapodistrian University of Athens, Athens 15771, Greece*; orcid.org/0000-0002-5166-8946

Purak Das − *Department of Chemistry, Missouri University of Science and Technology, Rolla, Missouri 65409, United States*

Lin Ai − *Department of Chemistry, Missouri University of Science and Technology, Rolla, Missouri 65409, United States; College of Chemistry, Beijing Normal University, Beijing 100875, People's Republic of China*; orcid.org/0000-0001-9721-1493

Yiannis Sanakis − *Institute of Advanced Materials, Physicochemical Processes, Nanotechnology and Microsystems, NCSR "Demokritos", Athens 15310, Greece*

Grigorios Raptopoulos − *Inorganic Chemistry Laboratory, Department of Chemistry, National and Kapodistrian University of Athens, Athens 15771, Greece*

Sudip Mohapatra − *Department of Chemistry, Missouri University of Science and Technology, Rolla, Missouri 65409, United States*

Amitava Choudhury − *Department of Chemistry, Missouri University of Science and Technology, Rolla, Missouri 65409, United States*; orcid.org/0000-0001-5496-7346

Zhicheng Sun − *Department of Chemistry, Center for Advanced Scientific Computing and Modeling (CASCaM), University of North Texas, Denton, Texas 76203, United States*

Complete contact information is available at: https://pubs.acs.org/10.1021/acs.organomet.1c00267

Notes

The authors declare no competing financial interest.

■ ACKNOWLEDGMENTS

This work was generously supported by the National Institute of General Medical Sciences of the National Institutes of Health under Award Numbers R15GM117508 and R15GM139071 (to P.S.), and in part by the National Science Foundation through grant CHE-0412959 (to P.S.). Authors Z.S. and T.R.C. further acknowledge the U.S. National Science Foundation for partial support of this research through grants CHE-1464943 and CHE-1953547. Authors G.R. and P.P. also thank the Special Account of Research Grants of the National and Kapodistrian University of Athens for partial support. We thank the reviewers for many insightful comments.

■ REFERENCES

(1) (a) *Aziridines and Epoxides in Organic Synthesis*; Yudin, A. K., Ed.; Wiley-VCH: Weinheim, 2006. (b) Padwa, A. Aziridines and Azirines: Monocyclic. In *Comprehensive Heterocyclic Chemistry III*; Katritzky, A. R., Ramsden, C. A., Scriven, E. F. V., Taylor, R. J. K., Eds.; Elsevier Science: Amsterdam, 2008; Vol. *1*, pp 1−104. (c) Sweeney, J. B. Aziridines: epoxides' ugly cousins? *Chem. Soc. Rev.* **2002**, *31*, 247−258. (d) Lapinsky, D. J. Three-Membered Ring Systems. *Prog. Heterocycl. Chem.* **2015**, *27*, 61−85. (e) Botuha, C.; Chemla, F.; Ferreira, F.; Pérez-Luna, A. Aziridines in Natural Product Synthesis. In *Heterocycles in Natural Product Synthesis*; Majumdar, K. C., Chattopadhyay, S. K., Eds.; Wiley-VCH: Weinheim, 2011; pp 1−39. (f) Padwa, A.; Murphree, S. S. Epoxides and aziridines − A mini review. *ARKIVOC* **2006**, *2006*, 6−33.

(2) (a) Ouyang, K.; Hao, W.; Zhang, W.-X.; Xi, Z. Transition-Metal-Catalyzed Cleavage of C−N Single Bonds. *Chem. Rev.* **2015**, *115*, 12045−12090. (b) Rotstein, B. H.; Zaretsky, S.; Rai, V.; Yudin, A. K. Small Heterocycles in Multicomponent Reactions. *Chem. Rev.* **2014**, *114*, 8323−8359. (c) Huang, C.-Y.; Doyle, A. G. The Chemistry of Transition Metals with Three-Membered Ring Heterocycles. *Chem. Rev.* **2014**, *114*, 8153−8198. (d) Stankovic, S.; D'hooghe, M.; Catak, S.; Eum, H.; Waroquier, M.; Van Speybroeck, V.; De Kimpe, N.; Ha, H.-J. Regioselectivity in the ring opening of non-activated aziridines. *Chem. Soc. Rev.* **2012**, *41*, 643−665. (e) Cardoso, A. L.; Pinho e Melo, T. M. V. D. Aziridines in Formal [3 + 2] Cycloadditions: Synthesis of Five-Membered Heterocycles. *Eur. J. Org. Chem.* **2012**, 6479−6501. (f) Lu, P. Recent developments in regioselective ring opening of aziridines. *Tetrahedron* **2010**, *66*, 2549−2560. (g) Schneider, C. Catalytic, Enantioselective Ring Opening of Aziridines. *Angew. Chem., Int. Ed.* **2009**, *48*, 2082−2084. (h) Hu, X. E. Nucleophilic ring opening of aziridines. *Tetrahedron* **2004**, *60*, 2701−2743. (i) McCoull, W.; Davis, F. A. Recent Synthetic Applications of Chiral Aziridines. *Synthesis* **2000**, *2000*, 1347−1365.

(3) (a) Tomasz, M.; Mitomycin, C. Small, fast and deadly (but very selective). *Chem. Biol.* **1995**, *2*, 575−579. (b) Coleman, R. S.; Li, J.; Navarro, A. Total Synthesis of Azinomycin A. *Angew. Chem., Int. Ed.* **2001**, *40*, 1736−1739. (c) Zhao, Q.; He, Q.; Ding, W.; Tang, M.; Kang, Q.; Yu, Y.; Deng, W.; Zhang, Q.; Fang, J.; Tang, G.; Liu, W. Characterization of the Azinomycin B Biosynthetic Gene Cluster Revealing a Different Iterative Type I Polyketide Synthase for Naphthoate Biosynthesis. *Chem. Biol.* **2008**, *15*, 693−705. (d) Ogasawara, Y.; Liu, H.-W. Biosynthetic Studies of Aziridine Formation in Azicemicins. *J. Am. Chem. Soc.* **2009**, *131*, 18066−18068. (e) Nakao, Y.; Fujita, M.; Warabi, K.; Matsunaga, S.; Fusetani, N. Miraziridine A, a Novel Cysteine Protease Inhibitor from the Marine Sponge *Theonella* aff. *Mirabilis*. *J. Am. Chem. Soc.* **2000**, *122*, 10462−10463. (f) Liu, Y.; Li, M.; Mu, H.; Song, S.; Zhang, Y.; Chen, K.; He, X.; Wang, H.; Dai, Y.; Lu, F.; Yan, Z.; Zhang, H. Identification and characterization of the ficellomycin biosynthesis gene cluster from *Streptomyces ficellus*. *Appl. Microbiol. Biotechnol.* **2017**, *101*, 7589−7602. (g) Foulke-Abel, J.; Agbo, H.; Zhang, H.; Mori, S.; Watanabe, C. M. H. Mode of action and biosynthesis of the azabicycle-containing natural products azinomycin and ficellomycin. *Nat. Prod. Rep.* **2011**, *28*, 693−704.

(4) (a) Ismail, F. M. D.; Levitsky, D. O.; Dembitsky, V. M. Aziridine alkaloids as potential therapeutic agents. *Eur. J. Med. Chem.* **2009**, *44*, 3373−3387. (b) Ballereau, S.; Andrieu-Abadie, N.; Saffon, N.; Génisson, Y. Synthesis and biological evaluation of aziridine-containing analogs of phytosphingosine. *Tetrahedron* **2011**, *67*, 2570−2578. (c) Dorr, R. T.; Wisner, L.; Samulitis, B. K.; Landowski, T. H.; Remers, W. A. Anti-tumor activity and mechanism of action for a cyanoaziridine-derivative, AMP423. *Cancer Chemother. Pharmacol.* **2012**, *69*, 1039−1049. (d) Pillai, B.; Cherney, M. M.; Diaper, C. M.; Sutherland, A.; Blanchard, J. S.; Vederas, J. C.; James, M. N. G. Structural insights into stereochemical inversion by diaminopimelate epimerase: An antibacterial drug target. *Proc. Natl. Acad. Sci. U. S. A.* **2006**, *103*, 8668−8673.

(5) (a) Ujjain, S. K.; Bhatia, R.; Ahuja, P. Aziridine-functionalized graphene: Effect of aromaticity for aryl functional groups on enhanced power conversion efficiency of organic photovoltaic cells. *J. Saudi Chem. Soc.* **2019**, *23*, 655−665. (b) Tuci, G.; Filippi, J.; Ba, H.; Rossin, A.; Luconi, L.; Pham-Huu, C.; Vizza, F.; Giambastiani, G. How to teach an old dog new (electrochemical) tricks: aziridine-functionalized CNTs as efficient electrocatalysts for the selective CO_2 reduction to CO. *J. Mater. Chem. A* **2018**, *6*, 16382−16389. (c) Moon, H. K.; Kang, S.; Yoon, H. J.

Aziridine-functionalized polydimethylsiloxanes for tailorable polymeric scaffolds: aziridine as a clickable moiety for structural modification of materials. *Polym. Chem.* **2017**, *8*, 2287−2291. (d) Tuci, G.; Luconi, L.; Rossin, A.; Berretti, E.; Ba, H.; Innocenti, M.; Yakhvarov, D.; Caporali, S.; Pham-Huu, C.; Giambastiani, G. Aziridine-Functionalized Multi-walled Carbon Nanotubes: Robust and Versatile Catalysts for the Oxygen Reduction Reaction and Knoevenagel Condensation. *ACS Appl. Mater. Interfaces* **2016**, *8*, 30099−30106. (e) Chen, R.; Chen, J. S.; Zhang, C.; Kessler, M. R. Rapid room-temperature polymerization of bio-based multiaziridine-containing compounds. *RSC Adv.* **2015**, *5*, 1557−1563. (f) Kim, H.-J.; Chaikittisilp, W.; Jang, K.-S.; Didas, S. A.; Johnson, J. R.; Koros, W. J.; Nair, S.; Jones, C. W. Aziridine-Functionalized Mesoporous Silica Membranes on Polymeric Hollow Fibers: Synthesis and Single-Component CO_2 and N_2 Permeation Properties. *Ind. Eng. Chem. Res.* **2015**, *54*, 4407−4413.

(6) (a) Degennaro, L.; Trinchera, P.; Luisi, R. Recent Advances in the Stereoselective Synthesis of Aziridines. *Chem. Rev.* **2014**, *114*, 7881−7929. (b) Pellissier, H. Recent Developments in Asymmetric Aziridination. *Adv. Synth. Catal.* **2014**, *356*, 1899−1935. (c) Pellissier, H. Recent developments in asymmetric aziridination. *Tetrahedron* **2010**, *66*, 1509−1555. (d) Singh, G. S.; D'hooghe, M.; De Kimpe, N. Synthesis and Reactivity of *C*-Heteroatom-Substituted Aziridines. *Chem. Rev.* **2007**, *107*, 2080−2135. (e) Watson, I. D. G.; Yu, L.; Yudin, A. K. Advances in Nitrogen Transfer Reactions Involving Aziridines. *Acc. Chem. Res.* **2006**, *39*, 194−206. (f) Osborn, H. M. I.; Sweeney, J. The asymmetric synthesis of aziridines. *Tetrahedron: Asymmetry* **1997**, *8*, 1693−1715. (g) Tanner, D. Chiral Aziridines−Their Synthesis and Use in Stereoselective Transformations. *Angew. Chem., Int. Ed. Engl.* **1994**, *33*, 599−619.

(7) (a) Darses, B.; Rodrigues, R.; Neuville, L.; Mazurais, M.; Dauban, P. Transition metal-catalyzed iodine(III)-mediated nitrene transfer reactions: efficient tools for challenging syntheses. *Chem. Commun.* **2017**, *53*, 493−508. (b) Chang, J. W. W.; Ton, T. M. U.; Chan, P. W. H. Transition-metal-catalyzed aminations and aziridinations of C−H and C═C bonds with iminoiodinanes. *Chem. Rec.* **2011**, *11*, 331−357. (c) Karila, D.; Dodd, R. H. Recent Progress in Iminoiodane-Mediated Aziridination of Olefins. *Curr. Org. Chem.* **2011**, *15*, 1507−1538.

(8) (a) Chanda, B. M.; Vyas, R.; Landge, S. S. Synthesis of aziridines using new catalytic systems with bromamine-T as the nitrene source. *J. Mol. Catal. A: Chem.* **2004**, *223*, 57−60. (b) Chanda, B. M.; Vyas, R.; Bedekar, A. V. Investigations in the Transition Metal catalyzed Aziridination of Olefins, Amination, and Other Insertion Reactions with Bromamine-T as the Source of Nitrene. *J. Org. Chem.* **2001**, *66*, 30−34.

(9) (a) Ma, Z.; Zhou, Z.; Kürti, L. Direct and Stereospecific Synthesis of N-H and N-Alkyl Aziridines from Unactivated Olefins Using Hydroxylamine-O-Sulfonic Acids. *Angew. Chem., Int. Ed.* **2017**, *56*, 9886−9890. (b) Jat, J. L.; Paudyal, M. P.; Gao, H.; Xu, Q.-L.; Yousufuddin, M.; Devarajan, D.; Ess, D. H.; Kürti, L.; Falck, J. R. Direct Stereospecific Synthesis of Unprotected N-H and N-Me Aziridines from Olefins. *Science* **2014**, *343*, 61−65. (c) Lebel, H.; Huard, K.; Lectard, S. *N*-Tosyloxycarbamates as a Source of Metal Nitrenes: Rhodium-Catalyzed C−H Insertion and Aziridination Reactions. *J. Am. Chem. Soc.* **2005**, *127*, 14198−14199.

(10) (a) Driver, T. G. Recent advances in transition metal-catalyzed *N*-atom transfer reactions of azides. *Org. Biomol. Chem.* **2010**, *8*, 3831−3846. (b) Intrieri, D.; Zardi, P.; Caselli, A.; Gallo, E. Organic azides: *"energetic reagents"* for the *inter*molecular amination of C−H bonds. *Chem. Commun.* **2014**, *50*, 11440−11453.

(11) (a) Hao, W.; Wu, X.; Sun, J. Z.; Siu, J. C.; MacMillan, S. N.; Lin, S. Radical Redox-Relay Catalysis: Formal [3 + 2] Cycloaddition of *N*-Acylaziridines and Alkenes. *J. Am. Chem. Soc.* **2017**, *139*, 12141−12144. (b) Goossens, H.; Vervisch, K.; Catak, S.; Stanković, S.; D'hooghe, M.; De Proft, F.; Geerlings, P.; De Kimpe, N.; Waroquier, M.; Van Speybroeck, V. Reactivity of Activated versus Nonactivated 2-(Bromomethyl)aziridines with respect to Sodium Methoxide: A Combined Computational and Experimental Study. *J. Org. Chem.* **2011**, *76*, 8698−8709. (c) Li, L.; Zhang, J. Lewis Acid-catalyzed [3 + 2] Cycloaddition of Alkynes with N-Tosyl-aziridines via Carbon−Carbon Bond Cleavage: Synthesis of Highly Substituted 3-Pyrrolines. *Org. Lett.* **2011**, *13*, 5940−5943. (d) Dauban, P.; Dodd, R. H. PhI = NSes: A New Iminoiodinane Reagent for the Copper-Catalyzed Aziridination of Olefins. *J. Org. Chem.* **1999**, *64*, 5304−5307. (e) Alonso, D. A.; Andersson, P. G. Deprotection of Sulfonyl Aziridines. *J. Org. Chem.* **1998**, *63*, 9455−9461. (f) Bergmeier, S. C.; Seth, P. P. A general method for deprotection of *N*-toluenesulfonyl aziridines using sodium naphthalenide. *Tetrahedron Lett.* **1999**, *40*, 6181−6184. (g) Warner, D. L.; Hibberd, A. M.; Kalman, M.; Klapars, A.; Vedejs, E. *N*-Silyl Protecting Groups for Labile Aziridines: Application toward the Synthesis of *N*-H Aziridinomitosenes. *J. Org. Chem.* **2007**, *72*, 8519−8522.

(12) (a) Zhu, Y.; Wang, Q.; Cornwall, R. G.; Shi, Y. Organocatalytic Asymmetric Epoxidation and Aziridination of Olefins and Their Synthetic Applications. *Chem. Rev.* **2014**, *114*, 8199−8256. (b) Zhang, Y.; Lu, Z.; Wulff, W. D. Catalytic Asymmetric Aziridination with Catalysts Derived from VAPOL and VANOL. *Synlett* **2009**, *2009*, 2715−2739. (c) Yoshimura, A.; Middleton, K. R.; Zhu, C.; Nemykin, V. N.; Zhdankin, V. V. Hypoiodite-Mediated Metal-Free catalytic Aziridination of Alkenes. *Angew. Chem., Int. Ed.* **2012**, *51*, 8059−8062. (d) Siu, T.; Yudin, A. K. Practical Olefin Aziridination with a Broad Substrate Scope. *J. Am. Chem. Soc.* **2002**, *124*, 530−531.

(13) (a) Chandrachud, P. P.; Jenkins, D. M. Transition Metal Aziridination Catalysts. In *Encyclopedia of Inorganic and Bioinorganic Chemistry*; Wiley Online Library, 2017; pp 1−11. (b) Che, C.-M.; Lo, V. K.-Y.; Zhou, C.-Y. Oxidation by Metals (Nitrene). In *Comprehensive Organic Synthesis II*, 2nd ed.; Knochel, P., Molander, G. A., Eds.; Elsevier: Amsterdam, 2014; Vol. 7, pp 26−85. (c) Jung, N.; Bräse, S. New Catalysts for the Transition-Metal-Catalyzed Synthesis of Aziridines. *Angew. Chem., Int. Ed.* **2012**, *51*, 5538−5540. (d) Jiang, H.; Zhang, X. P. Oxidation: C−N Bond Formation by Oxidation (Aziridines). In *Comprehensive Chirality*; Carreira, E. M., Yamamoto, H., Eds.; Elsevier: Amsterdam, 2012; Vol. 5, pp 168−182. (e) Mößner, C.; Bolm, C. Catalyzed Asymmetric Aziridinations. In *Transition Metals for Organic Synthesis*, 2nd ed.; Beller, M., Bolm, C., Eds.; Wiley-VCH: Weinheim, Germany, 2004; pp 389−402. (f) Halfen, J. A. Recent Advances in Metal-Mediated Carbon-Nitrogen Bond Formation Reactions: Aziridination and Amidation. *Curr. Org. Chem.* **2005**, *9*, 657−669. (g) Müller, P.; Fruit, C. Enantioselective Catalytic Aziridinations and Asymmetric Nitrene Insertions into CH Bonds. *Chem. Rev.* **2003**, *103*, 2905−2919.

(14) Historic Mn/Fe porphyrinoid systems: (a) Mansuy, D.; Mahy, J.-P.; Dureault, A.; Bedi, G.; Battioni, P. Iron- and manganese-porphyrin catalysed aziridination of alkenes by tosyl- and acyl-iminoiodobenzene. *J. Chem. Soc., Chem. Commun.* **1984**, 1161−1163. (b) Mahy, J.-P.; Battioni, P.; Mansuy, D. Formation of an Iron(III) Porphyrin Complex with a Nitrene Moiety Inserted into a Fe−N Bond during Alkene Aziridination by [(Tosylimido)iodo]benzene Catalyzed by Iron(III) Porphyrins. *J. Am. Chem. Soc.* **1986**, *108*, 1079−1080. (c) Mahy, J.-P.; Bedi, G.; Battioni, P.; Mansuy, D. Aziridination of alkenes catalysed by porphyrinirons: Selection of catalysts for optimal efficiency and stereospecificity. *J. Chem. Soc., Perkin Trans. 2* **1988**, *2*, 1517−1524. (d) Groves, J. T.; Takahashi, T. Activation and Transfer of Nitrogen from Nitridomanganese(V) Porphyrin Complex. The Aza Analogue of Epoxidation. *J. Am. Chem. Soc.* **1983**, *105*, 2073−2074.

(15) For select reviews of metal porphyrinoid nitrene-transfer systems, see: (a) Intrieri, D.; Carminati, D. M.; Gallo, E. Recent Advances in Metal Porphyrinoid-Catalyzed Nitrene and Carbene Transfer Reactions. In *Handbook of Porphyrin Science*; Kadish, K. M., Smith, K. M., Guilard, R., Eds.; World Scientific, 2016; Vol. *38*, pp 1−99. (b) Anding, B. J.; Woo, L. K. An Overview of Metalloporphyrin-Catalyzed Carbon and Nitrogen Group Transfer Reactions. In *Handbook of Porphyrin Science*; Kadish, K. M., Smith, K. M., Guilard, R., Eds.; World Scientific, 2012; Vol. *21*, pp 145−319. (c) Ruppel, J. V.; Fields, K. B.; Snyder, N. L.; Zhang, X. P. Metalloporphyrin-Catalyzed Asymmetric Atom/Group Transfer Reactions. In *Handbook of Porphyrin Science*; Kadish, K. M., Smith, K. M., Guilard, R., Eds.; World Scientific, 2010; Vol. *10*, pp 1−84. (d) Fantauzzi, S.; Caselli, A.;

https://doi.org/10.1021/acs.organomet.1c00267
Organometallics 2021, 40, 1974−1996

Gallo, E. Nitrene transfer reactions mediated by metallo-porphyrin complexes. *Dalton Trans.* **2009**, 5434−5443.
(16) For select reviews of engineered hemoproteins for nitrene transfer to alkenes, see: (a) Brandenberg, O. F.; Fasan, R.; Arnold, F. H. Exploiting and engineering hemoproteins for abiological carbene and nitrene transfer reactions. *Curr. Opin. Biotechnol.* **2017**, *47*, 102−111. (b) Farwell, C. C.; Zhang, R. K.; McIntosh, J. A.; Hyster, T. K.; Arnold, F. H. Enantioselective Enzyme-Catalyzed Aziridination Enabled by Active-Site Evolution of a Cytochrome P450. *ACS Cent. Sci.* **2015**, *1*, 89−93. (c) Gober, J. G.; Brustad, E. M. Non-natural carbenoid and nitrenoid insertion reactions catalyzed by heme proteins. *Curr. Opin. Chem. Biol.* **2016**, *35*, 124−132.
(17) For select examples of Mn-based nitrene-transfer to alkenes, see: (a) Zdilla, M. J.; Abu-Omar, M. M. Mechanism of Catalytic Aziridination with Manganese Corrole: The Often Postulated High-Valent Mn(V) Imido Is Not the Group Transfer Reagent. *J. Am. Chem. Soc.* **2006**, *128*, 16971−16979. (b) Nishikori, H.; Katsuki, T. Catalytic and highly enantioselective aziridination of styrene derivatives. *Tetrahedron Lett.* **1996**, *37*, 9245−9248. (c) Minakata, S.; Ando, T.; Nishimura, M.; Ryu, I.; Komatsu, M. Novel Asymmetric and Stereospecific Aziridination of Alkenes with a Chiral Nitridomanganese Complex. *Angew. Chem., Int. Ed.* **1998**, *37*, 3392−3394. (d) Du Bois, J.; Tomooka, C. S.; Hong, J.; Carreira, E. M. Nitridomanganese(V) Complexes: Design, Preparation, and Use as Nitrogen Atom-Transfer Reagents. *Acc. Chem. Res.* **1997**, *30*, 364−372. (e) Lai, T.-S.; Kwong, H.-L.; Che, C.-M.; Peng, S.-M. Catalytic and asymmetric aziridination of alkenes catalyzed by a chiral manganese porphyrin complex. *Chem. Commun.* **1997**, 2373−2374. (f) Liang, J.-L.; Huang, J.-S.; Yu, X.-Q.; Zhu, N.; Che, C.-M. Metalloporphyrin-Mediated Asymmetric Nitrogen-Atom Transfer to Hydrocarbons: Aziridination of Alkenes and Amidation of Saturated C−H Bonds Catalyzed by Chiral Ruthenium and Manganese Porphyrins. *Chem. - Eur. J.* **2002**, *8*, 1563−1572. (g) O'Connor, K. J.; Wey, S.-J.; Burrows, C. J. Alkene aziridination and epoxidation catalyzed by chiral metal salen complexes. *Tetrahedron Lett.* **1992**, *33*, 1001−1004.
(18) For select examples of Fe-based nitrene-transfer to alkenes, see: (a) Damiano, C.; Intrieri, D.; Gallo, E. Aziridination of alkenes promoted by iron or ruthenium complexes. *Inorg. Chim. Acta* **2018**, *470*, 51−67. (b) Fingerhut, A.; Serdyuk, O. V.; Tsogoeva, S. B. *Non-heme iron* catalysts for epoxidation and aziridination reactions of challenging terminal alkenes: towards sustainability. *Green Chem.* **2015**, *17*, 2042−2058. (c) Correa, A.; Mancheño, O. G.; Bolm, C. Iron-catalysed carbon-heteroatom and heteroatom-heteroatom bond forming processes. *Chem. Soc. Rev.* **2008**, *37*, 1108−1117. (d) Iovan, D. A.; Betley, T. A. Characterization of Iron-Imido Species Relevant for *N*-Group Transfer Chemistry. *J. Am. Chem. Soc.* **2016**, *138*, 1983−1993. (e) Hennessy, E. T.; Liu, R. Y.; Iovan, D. A.; Duncan, R. A.; Betley, T. A. Iron-mediated intermolecular N-group transfer chemistry with olefinic substrates. *Chem. Sci.* **2014**, *5*, 1526−1532. (f) King, E. R.; Hennessy, E. T.; Betley, T. A. Catalytic C−H Bond Amination from High-Spin Iron Imido Complexes. *J. Am. Chem. Soc.* **2011**, *133*, 4917−4923. (g) Patra, R.; Coin, G.; Castro, L.; Dubourdeaux, P.; Clémancey, M.; Pécaut, J.; Lebrun, C.; Maldivi, P.; Latour, J.-M. Rational design of Fe catalysts for olefin aziridination through DFT-based mechanistic analysis. *Catal. Sci. Technol.* **2017**, *7*, 4388−4400. (h) Avenier, F.; Latour, J.-M. Catalytic aziridination of olefins and amidation of thioanisole by a non-heme iron complex. *Chem. Commun.* **2004**, 1544−1545. (i) Liu, Y.; Che, C. M. $[Fe^{III}(F_{20}\text{-tpp})Cl]$ Is an Effective Catalyst for Nitrene Transfer Reactions and Amination of Saturated Hydrocarbons with Sulfonyl and Aryl Azides as Nitrogen Source under Thermal and Microwave-Assisted Conditions. *Chem. - Eur. J.* **2010**, *16*, 10494−10501. (j) Klotz, K. L.; Slominski, L. M.; Hull, A. V.; Gottsacker, V. M.; Mas-Ballesté, R.; Que, L., Jr.; Halfen, J. A. Non-heme iron(II) complexes are efficient olefin aziridination catalysts. *Chem. Commun.* **2007**, 2063−2065. (k) Klotz, K. L.; Slominski, L. M.; Riemer, M. E.; Phillips, J. A.; Halfen, J. A. Mechanism of the Iron-Mediated Alkene Aziridination reaction: Experimental and Computational Investigations. *Inorg. Chem.* **2009**, *48*, 801−803. (l) Chandrachud, P. P.; Bass, H. M.; Jenkins, D. M. Synthesis of Fully Aliphatic Aziridines with a Macrocycle Tetracarbene Iron Catalyst. *Organometallics* **2016**, *35*, 1652−1657. (m) Cramer, S. A.; Jenkins, D. M. Synthesis of Aziridines from Alkenes and Aryl Azides with a Reusable Macrocyclic Tetracarbene Iron Catalyst. *J. Am. Chem. Soc.* **2011**, *133*, 19342−19345. (n) Muñoz, S. B., Jr.; Lee, W.-T.; Dickie, D. A.; Scepaniak, J. J.; Subedi, D.; Pink, M.; Johnson, M. D.; Smith, J. M. Styrene Aziridination by Iron(IV) Nitrides. *Angew. Chem., Int. Ed.* **2015**, *54*, 10600−10603. (o) Nakanishi, M.; Salit, A.-F.; Bolm, C. Iron-Catalyzed Aziridination Reactions. *Adv. Synth. Catal.* **2008**, *350*, 1835−1840. (p) Mayer, A. C.; Salit, A.-F.; Bolm, C. Iron-catalysed aziridination reactions promoted by an ionic liquid. *Chem. Commun.* **2008**, 5975−5977. (q) Heuss, B. D.; Mayer, M. F.; Dennis, S.; Hossain, M. M. Iron mediated nitrenoid transfer: $[(\eta^5\text{-}C_5H_5)Fe(CO)_2(THF)]^+[BF_4]^-$ catalyzed aziridination of olefins. *Inorg. Chim. Acta* **2003**, *342*, 301−304.
(19) For select examples of Co-based nitrene-transfer to alkenes, see: (a) Jiang, H.; Lang, K.; Lu, H.; Wojtas, L.; Zhang, X. P. Asymmetric Radical Bicyclization of Allyl Azidoformates via Cobalt(II)-Based Metalloradical Catalysis. *J. Am. Chem. Soc.* **2017**, *139*, 9164−9167. (b) Jiang, H.; Lang, K.; Lu, H.; Wojtas, L.; Zhang, X. P. Intramolecular Radical Aziridination of Allylic Sulfamoyl Azides by Cobalt(II)-Based Metalloradical Catalysis: Effective Construction of Strained Heterobicyclic Structures. *Angew. Chem., Int. Ed.* **2016**, *55*, 11604−11608. (c) Subbarayan, V.; Jin, L.-M.; Cui, X.; Zhang, X. P. Room temperature activation of aryloxysulfonyl azides by [Co(II)(TPP)] for selective radical aziridination of alkenes via metalloradical catalysis. *Tetrahedron Lett.* **2015**, *56*, 3431−3434. (d) Tao, J.; Jin, L.-M.; Zhang, X. P. Synthesis of chiral N-phosphoryl aziridines through enantioselective aziridination of alkenes with phosphoryl azide via Co(II)-based metalloradical catalysis. *Beilstein J. Org. Chem.* **2014**, *10*, 1282−1289. (e) Jin, L.-M.; Xu, X.; Lu, H.; Cui, X.; Wojtas, L.; Zhang, X. P. Effective Synthesis of Chiral *N*-Fluoroaryl Aziridines through Enantioselective Aziridination of Alkenes with Fluoroaryl Azides. *Angew. Chem., Int. Ed.* **2013**, *52*, 5309−5313. (f) Suarez, A. I. O.; Jiang, H.; Zhang, X. P.; de Bruin, B. The radical mechanism of cobalt(II) porphyrin-catalyzed olefin aziridination and the importance of cooperative H-bonding. *Dalton Trans.* **2011**, *40*, 5697−5705. (g) Lu, H.; Jiang, H.; Hu, Y.; Wojtas, L.; Zhang, X. P. Chemoselective intramolecular allylic C−H amination *versus* C=C aziridination through Co(II)-based metalloradical catalysis. *Chem. Sci.* **2011**, *2*, 2361−2366. (h) Subbarayan, V.; Ruppel, J. V.; Zhu, S.; Perman, J. A.; Zhang, X. P. Highly asymmetric cobalt-catalyzed aziridination of alkenes with trichloroethoxysulfonyl azide ($TcesN_3$). *Chem. Commun.* **2009**, 4266−4268. (i) Jones, J. E.; Ruppel, J. V.; Gao, G.-Y.; Moore, T. M.; Zhang, X. P. Cobalt-Catalyzed Asymmetric Olefin Aziridination with Diphenylphosphoryl Azide. *J. Org. Chem.* **2008**, *73*, 7260−7265. (j) Ruppel, J. V.; Jones, J. E.; Huff, C. A.; Kamble, R. M.; Chen, Y.; Zhang, X. P. A Highly Effective Cobalt Catalyst for Olefin Aziridination with Azides: Hydrogen Bonding Guided Catalyst Design. *Org. Lett.* **2008**, *10*, 1995−1998. (k) Gao, G.-Y.; Jones, J. E.; Vyas, R.; Harden, J. D.; Zhang, X. P. Cobalt-Catalyzed Aziridination with Diphenylphosphoryl Azide (DPPA): Direct Synthesis of *N*-Phosphorus-Substituted Aziridines from Alkenes. *J. Org. Chem.* **2006**, *71*, 6655−6658. (l) Gao, G.-Y.; Harden, J. D.; Zhang, X. P. Cobalt-Catalyzed Efficient Aziridination of Alkenes. *Org. Lett.* **2005**, *7*, 3191−3193. (m) Caselli, A.; Gallo, E.; Fantauzzi, S.; Morlacchi, S.; Ragaini, F.; Cenini, S. Allylic Amination and Aziridination of Olefins by Aryl Azides Catalyzed by Co^{II}(tpp): A Synthetic and Mechanistic Study. *Eur. J. Inorg. Chem.* **2008**, *2008*, 3009−3019. (n) Caselli, A.; Gallo, E.; Ragaini, F.; Ricatto, F.; Abbiati, G.; Cenini, S. Chiral porphyrin complexes of cobalt(II) and ruthenium(II) in catalytic cyclopropanation and amination reactions. *Inorg. Chim. Acta* **2006**, *359*, 2924−2932. (o) Cenini, S.; Tollari, S.; Penoni, A.; Cereda, C. Catalytic amination of unsaturated hydrocarbons: reactions of p-nitrophenylazide with alkenes catalyzed by metallo-porphyrins. *J. Mol. Catal. A: Chem.* **1999**, *137*, 135−146.
(20) For select examples of Ni-based nitrene-transfer to alkenes, see: (a) Waterman, R.; Hillhouse, G. L. Group Transfer from Nickel Imido, Phosphinidine, and Carbene Complexes to Ethylene with Formation of Aziridine, Phosphirane, and Cyclopropane Products. *J. Am. Chem. Soc.* **2003**, *125*, 13350−13351. (b) Lin, B. L.; Clough, C. R.; Hillhouse, G. L.

https://doi.org/10.1021/acs.organomet.1c00267
Organometallics 2021, 40, 1974−1996

Interactions of Aziridines with Nickel Complexes: Oxidative-Addition and Reductive-Elimination Reactions that Break and Make C−N Bonds. *J. Am. Chem. Soc.* **2002**, *124*, 2890−2891.

(21) For historic examples of Cu-based enantioselective aziridinations, see: (a) Li, Z.; Quan, R. W.; Jacobsen, E. N. Mechanism of the (Diimine)copper-Catalyzed Asymmetric Aziridination of Alkenes. Nitrene Transfer via Ligand-Accelerated Catalysis. *J. Am. Chem. Soc.* **1995**, *117*, 5889−5890. (b) Li, Z.; Conser, K. R.; Jacobsen, E. N. Asymmetric Alkene Aziridination with Readily Available Chiral Diimine-Based Catalysts. *J. Am. Chem. Soc.* **1993**, *115*, 5326−5327. (c) Evans, D. A.; Faul, M. M.; Bilodeau, M. T.; Anderson, B. A.; Barnes, D. M. Bis(oxazoline)-copper complexes as chiral catalysts for the enantioselective aziridination of olefins. *J. Am. Chem. Soc.* **1993**, *115*, 5328−5329.

(22) For select examples of Cu-based nitrene-transfer to alkenes, see: (a) Gephart, R. T., III; Warren, T. H. Copper-Catalyzed sp^3 C−H Amination. *Organometallics* **2012**, *31*, 7728−7752. (b) Lebel, H.; Parmentier, M. Copper-catalyzed enantioselective aziridination of styrenes. *Pure Appl. Chem.* **2010**, *82*, 1827−1833. (c) Lebel, H.; Parmentier, M.; Leogane, O.; Ross, K.; Spitz, C. Copper bis(oxazolines) as catalysts for stereoselective aziridination of styrenes with *N*-tosyloxycarbamates. *Tetrahedron* **2012**, *68*, 3396−3409. (d) Maestre, L.; Sameera, W. M. C.; Díaz-Requejo, M. M.; Maseras, F.; Pérez, P. J. A General Mechanism for the Copper- and Silver-Catalyzed Olefin Aziridination Reactions: Concomitant Involvement of the Singlet and Triplet Pathways. *J. Am. Chem. Soc.* **2013**, *135*, 1338−1348. (e) Mairena, M. A.; Díaz-Requejo, M. M.; Belderraín, T. R.; Nicasio, M. C.; Trofimenko, S.; Pérez, P. J. Copper-Homoscorpionate Complexes as Very Active Catalysts for the Olefin Aziridination Reaction. *Organometallics* **2004**, *23*, 253−256. (f) Díaz-Requejo, M. M.; Pérez, P. J.; Brookhart, M.; Templeton, J. L. Substituent Effects on the Reaction Rates of Copper-Catalyzed Cyclopropanation and Aziridination of para-Substituted Styrenes. *Organometallics* **1997**, *16*, 4399−4402. (g) Bagchi, V.; Paraskevopoulou, P.; Das, P.; Chi, L.; Wang, Q.; Choudhury, A.; Mathieson, J. S.; Cronin, L.; Pardue, D. B.; Cundari, T. R.; Mitrikas, G.; Sanakis, Y.; Stavropoulos, P. A Versatile Tripodal Cu(I) Reagent for C−N Bond Construction via Nitrene-Transfer Chemistry: Catalytic Perspectives and Mechanistic Insights on C−H Aminations/Amidinations and Olefin Aziridinations. *J. Am. Chem. Soc.* **2014**, *136*, 11362−11381. (h) Lam, T. L.; Tso, K. C.-H.; Cao, B.; Yang, C.; Chen, D.; Chang, X.-Y.; Huang, J.-S.; Che, C.-M. Tripodal S-Ligand Complexes of Copper(I) as Catalysts for Alkene Aziridination, Sulfide Sulfimidation, and C−H Amination. *Inorg. Chem.* **2017**, *56*, 4253−4257. (i) Li, Y.; He, J.; Khankhoje, V.; Herdtweck, E.; Köhler, K.; Storcheva, O.; Cokoja, M.; Kühn, F. E. Copper(II) complexes incorporating poly/perfluorinated alkoxyaluminate-type weakly coordinating anions: Syntheses, characterization and catalytic application in stereoselective olefin aziridination. *Dalton Trans.* **2011**, *40*, 5746−5754. (j) Comba, P.; Haaf, C.; Lienke, A.; Muruganantham, A.; Wadepohl, H. Synthesis, Structure, and Highly Efficient Copper-Catalyzed Aziridination with a Tetraaza-Bispidine Ligand. *Chem. - Eur. J.* **2009**, *15*, 10880−10887. (k) Wang, X.; Ding, K. One-Pot Enantioselective Aziridination of Olefins Catalyzed by a Copper(I) Complex of a Novel Diimine Ligand by Using $PhI(OAc)_2$ and Sulfonamide as Nitrene Precursors. *Chem. - Eur. J.* **2006**, *12*, 4568−4575. (l) Robert-Peillard, F.; Di Chenna, P. H.; Liang, C.; Lescot, C.; Collet, F.; Dodd, R. H.; Dauban, P. Catalytic stereoselective alkene aziridination with sulfonimidamides. *Tetrahedron: Asymmetry* **2010**, *21*, 1447−1457. (m) Kundu, S.; Miceli, E.; Farquhar, E.; Pfaff, F. F.; Kuhlmann, U.; Hildebrandt, P.; Braun, B.; Greco, C.; Ray, K. Lewis Acid Trapping of an Elusive Copper−Tosylnitrene Intermediate Using Scandium Triflate. *J. Am. Chem. Soc.* **2012**, *134*, 14710−14713. (n) Ma, L.; Jiao, P.; Zhang, Q.; Du, D.-M.; Xu, J. Ligand and substrate π-stacking interaction controlled enantioselectivity in the asymmetric aziridination. *Tetrahedron: Asymmetry* **2007**, *18*, 878−884. (o) Vedernikov, A. N.; Caulton, K. G. Angular Ligand Constraint Yields an Improved Olefin Aziridination Catalyst. *Org. Lett.* **2003**, *5*, 2591−2594. (p) Evans, D. A.; Faul, M. M.; Bilodeau, M. T. Development of the Copper-Catalyzed Olefin Aziridination Reaction. *J. Am. Chem. Soc.* **1994**, *116*, 2742−2753. (q) Kwart, H.; Khan, A. A. Copper-Catalyzed Decomposition of Benzenesulfonyl Azide in Cyclohexene Solution. *J. Am. Chem. Soc.* **1967**, *89*, 1951−1953.

(23) For select examples of Ru-based nitrene-transfer to alkenes, see: (a) Uchida, T.; Katsuki, T. Asymmetric Nitrene Transfer Reactions: Sulfimidation, Aziridination and C−H Amination Using Azide Compounds as Nitrene Precursors. *Chem. Rec.* **2014**, *14*, 117−129. (b) Kim, C.; Uchida, T.; Katsuki, T. Asymmetric olefin aziridination using a newly designed Ru(CO)(salen) complex as the catalyst. *Chem. Commun.* **2012**, *48*, 7188−7190. (c) Kawabata, H.; Omura, K.; Uchida, T.; Katsuki, T. Construction of Robust Ruthenium(salen)(CO) Complexes and Asymmetric Aziridination with Nitrene Precursors in the Form of Azide Compounds That Bear Easily Removable *N*-Sulfonyl Groups. *Chem. - Asian J.* **2007**, *2*, 248−256. (d) Harvey, M. E.; Musaev, D.; Du Bois, J. A Diruthenium Catalyst for Selective, Intramolecular Allylic C−H Amination: Reaction Development and Mechanistic Insight Gained through Experiment and Theory. *J. Am. Chem. Soc.* **2011**, *133*, 17207−17216. (e) Chan, K.-H.; Guan, X.; Lo, V. K.-Y.; Che, C.-M. Elevated Catalytic Activity of Ruthenium(II)−Porphyrin-Catalyzed Carbene/Nitrene Transfer and Insertion Reactions with N-Heterocyclic Carbene Ligands. *Angew. Chem., Int. Ed.* **2014**, *53*, 2982−2987. (f) Leung, S. K.-Y.; Tsui, W.-M.; Huang, J.-S.; Che, C.-M.; Liang, J.-L.; Zhu, N. Imido Transfer from Bis(imido)ruthenium(VI) Porphyrins to Hydrocarbons: Effect of Imido Substituents, C−H Bond Dissociation Energies, and $Ru^{VI/V}$ Reduction Potentials. *J. Am. Chem. Soc.* **2005**, *127*, 16629−16640. (g) Au, S.-M.; Huang, J.-S.; Yu, W.-Y.; Fung, W.-H.; Che, C.-M. Aziridination of Alkenes and Amidation of Alkanes by Bis(tosylimido)ruthenium(VI) Porphyrins. A Mechanistic Study. *J. Am. Chem. Soc.* **1999**, *121*, 9120−9132. (h) Fantauzzi, S.; Gallo, E.; Caselli, A.; Piangiolino, C.; Ragaini, F.; Re, N.; Cenini, S. Rearrangement of *N*-Aryl-2-Vinylaziridines to Benzoazepines and Dihydropyrroles: A Synthetic and Theoretical Study. *Chem. - Eur. J.* **2009**, *15*, 1241−1251. (i) Fantauzzi, S.; Gallo, E.; Caselli, A.; Piangiolino, C.; Ragaini, F.; Cenini, S. The (Porphyrin)ruthenium-Catalyzed Aziridination of Olefins Using Aryl Azides as Nitrogen Sources. *Eur. J. Org. Chem.* **2007**, *2007*, 6053−6059. (j) Fantauzzi, S.; Gallo, E.; Caselli, A.; Ragaini, F.; Macchi, P.; Casati, N.; Cenini, S. Origin of the Deactivation in Styrene Aziridination by Aryl Azides, Catalyzed by Ruthenium Porphyrin Complexes. Structural Characterization of a Δ^2-1,2,3-triazoline Ru^{II}(TPP)CO Complex. *Organometallics* **2005**, *24*, 4710−4713. (k) Zardi, P.; Pozzoli, A.; Ferretti, F.; Manca, G.; Mealli, C.; Gallo, E. A mechanistic investigation of the ruthenium porphyrin catalyzed aziridination of olefins by aryl azides. *Dalton Trans.* **2015**, *44*, 10479−10489. (l) Manca, G.; Gallo, E.; Intrieri, D.; Mealli, C. DFT Mechanistic Proposal of the Ruthenium Porphyrin-Catalyzed Allylic Amination by Organic Azides. *ACS Catal.* **2014**, *4*, 823−832.

(24) For select examples of Rh-based nitrene-transfer to alkenes, see ref 9 and the following: (a) Roizen, J. L.; Harvey, M. E.; Du Bois, J. Metal-Catalyzed Nitrogen-Atom Transfer Methods for the Oxidation of Aliphatic C−H Bonds. *Acc. Chem. Res.* **2012**, *45*, 911−922. (b) Fiori, K. W.; Espino, C. G.; Brodsky, B. H.; Du Bois, J. A mechanistic analysis of the Rh-catalyzed intramolecular C−H amination reaction. *Tetrahedron* **2009**, *65*, 3042−3051. (c) Fruit, C.; Robert-Peillard, F.; Bernardinelli, G.; Müller, P.; Dodd, R. H.; Dauban, P. Diastereoselective rhodium-catalyzed nitrene transfer starting from chiral sulfonimidamide-derived iminoiodanes. *Tetrahedron: Asymmetry* **2005**, *16*, 3484−3487. (d) Müller, P.; Baud, C.; Jacquier, Y. The rhodium(III)-catalyzed aziridination of olefins with {[(4-Nitrophenyl)-sulfonyl]imino}phenyl-λ^3-iodane. *Can. J. Chem.* **1998**, *76*, 738−750. (e) Nageli, I.; Baud, C.; Bernardinelli, G.; Jacquier, Y.; Moraon, M.; Mullet, P. Rhodium(II)-Catalyzed CH Insertions with {[(4-Nitrophenyl)-sulfonyl]imino}phenyl-λ^3-iodane. *Helv. Chim. Acta* **1997**, *80*, 1087−1105. (f) Catino, A. J.; Nichols, J. M.; Forslund, R. E.; Doyle, M. P. Efficient Aziridination of Olefins Catalyzed by Mixed-Valent Dirhodium(II, III) Caprolactamate. *Org. Lett.* **2005**, *7*, 2787−2790. (g) Liang, J.-L.; Yuan, S.-X.; Chan, P. W. H.; Che, C.-M. Rhodium-(II,II) Dimer as an Efficient Catalyst for Aziridination of Sulfonamides and Amidation of Steroids. *Org. Lett.* **2002**, *4*, 4507−4510.

https://doi.org/10.1021/acs.organomet.1c00267
Organometallics 2021, 40, 1974−1996

(25) For select examples of Pd-based nitrene-transfer to alkenes, see: (a) Okamoto, K.; Oda, T.; Kohigashi, S.; Ohe, K. Palladium-catalyzed Decarboxylative Intramolecular Aziridination from 4*H*-Isoxazol-5-ones Leading to 1-Azabicyclo[3.1.0]hex-2-enes. *Angew. Chem., Int. Ed.* **2011**, *50*, 11470−11473. (b) Han, J.; Li, Y.; Zhi, S.; Pan, Y.; Timmons, C.; Li, G. Palladium-catalyzed aziridination of alkenes using *N*,*N*-dichloro-p-toluenesulfonamide as nitrogen source. *Tetrahedron Lett.* **2006**, *47*, 7225−7228.

(26) For select examples of Ag-based nitrene-transfer to alkenes, see: (a) Mat Lani, A. S.; Schomaker, J. M. Site-Selective, Catalyst-Controlled Alkene Aziridination. *Synthesis* **2018**, *50*, 4462−4470. (b) Ju, M.; Weatherly, C. D.; Guzei, I. A.; Schomaker, J. M. Chemo- and Enantioselective Intramolecular Silver-Catalyzed Aziridinations. *Angew. Chem., Int. Ed.* **2017**, *56*, 9944−9948. (c) Dolan, N. S.; Scamp, R. J.; Yang, T.; Berry, J. F.; Schomaker, J. M. Catalyst-Controlled and Tunable, Chemoselective Silver-catalyzed Intermolecular Nitrene Transfer: Experimental and Computational Studies. *J. Am. Chem. Soc.* **2016**, *138*, 14658−14667. (d) Rigoli, J. W.; Weatherly, C. D.; Alderson, J. M.; Vo, B. T.; Schomaker, J. M. Tunable, Chemoselective Amination via Silver Catalysis. *J. Am. Chem. Soc.* **2013**, *135*, 17238−17241. (e) Huang, M.; Corbin, J. R.; Dolan, N. S.; Fry, C. G.; Vinokur, A. I.; Guzei, I. A.; Schomaker, J. M. Synthesis, Characterization, and Variable-Temperature NMR Studies of Silver(I) Complexes for Selective Nitrene Transfer. *Inorg. Chem.* **2017**, *56*, 6725−6733. (f) Weatherly, C.; Alderson, J. M.; Berry, J. F.; Hein, J. E.; Schomaker, J. M. Catalyst-Controlled Nitrene Transfer by Tuning Metal:Ligand Ratios: Inshight into the Mechanisms of Chemoselectivity. *Organometallics* **2017**, *36*, 1649−1661. (g) Scamp, R. J.; Rigoli, J. W.; Schomaker, J. M. Chemoselective silver-catalyzed nitrene insertion reactions. *Pure Appl. Chem.* **2014**, *86*, 381−393. (h) Rigoli, J. W.; Weatherly, C. D.; Vo, B. T.; Neale, S.; Meis, A. R.; Schomaker, J. M. Chemoselective Allene Aziridination via Ag(I) Catalysis. *Org. Lett.* **2013**, *15*, 290−293. (i) Llaveria, J.; Beltrán, A.; Díaz-Requejo, M. M.; Matheu, M. I.; Castillón, S.; Pérez, P. J. Efficient Silver-Catalyzed Regio- and Stereospecific Aziridination of Dienes. *Angew. Chem., Int. Ed.* **2010**, *49*, 7092−7095. (j) Li, Z.; He, C. Recent Advances in Silver-Catalyzed Nitrene, Carbene, and Silylene-Transfer Reactions. *Eur. J. Org. Chem.* **2006**, *2006*, 4313−4322. (k) Cui, Y.; He, C. Efficient Aziridination of Olefins Catalyzed by a Unique Disilver(I) Compound. *J. Am. Chem. Soc.* **2003**, *125*, 16202−16203.

(27) For select examples of Au-based nitrene-transfer to alkenes, see: (a) Li, Z.; Ding, X.; He, C. Nitrene Transfer Reactions Catalyzed by Gold Complexes. *J. Org. Chem.* **2006**, *71*, 5876−5880. (b) Deng, X.; Baker, T. A.; Friend, C. M. A Pathway for NH Addition to Styrene Promoted by Gold. *Angew. Chem., Int. Ed.* **2006**, *45*, 7075−7078.

(28) (a) Singh, R.; Mukherjee, A. Metalloporphyrin Catalyzed C−H Amination. *ACS Catal.* **2019**, *9*, 3604−3617. (b) Park, Y.; Kim, Y.; Chang, S. Transition Metal-Catalyzed C−H Amination: Scope, Mechanism, and Applications. *Chem. Rev.* **2017**, *117*, 9247−9301. (c) Stavropoulos, P. Metal-Catalyzed and Metal-Free Intermolecular Amination of Light Alkanes and Benzenes. *Comments Inorg. Chem.* **2017**, *37*, 1−57. (d) Hazelard, D.; Nocquet, P.-A.; Compain, P. Catalytic C−H amination at its limits: challenges and solutions. *Org. Chem. Front.* **2017**, *4*, 2500−2521. (e) Collet, F.; Lescot, C.; Dauban, P. Catalytic C−H amination: the stereoselectivity issue. *Chem. Soc. Rev.* **2011**, *40*, 1926−1936. (f) Zalatan, D. N.; Du Bois, J. Metal-Catalyzed Oxidations of C−H to C−N Bonds. *Top. Curr. Chem.* **2009**, *292*, 347−378. (g) Díaz-Requejo, M. M.; Pérez, P. J. Coinage Metal Catalyzed C−H Bond Functionalization of Hydrocarbons. *Chem. Rev.* **2008**, *108*, 3379−3394.

(29) Hu, L.; Chen, H. What Factors Control the Reactivity of Cobalt−Imido Complexes in C−H Bond Activation via Hydrogen Abstraction? *ACS Catal.* **2017**, *7*, 285−292.

(30) (a) Jones, C.; Schulten, C.; Rose, R. P.; Stasch, A.; Aldridge, S.; Woodul, W. D.; Murray, K. S.; Moubaraki, B.; Brynda, M.; La Macchia, G.; Gagliardi, L. Amidinato− and Guanidinato−Cobalt(I) Complexes: Characterization of Exceptionally Short Co−Co Interactions. *Angew. Chem., Int. Ed.* **2009**, *48*, 7406−7410. (b) Cowley, R. E.; Bontchev, R. P.; Sorrell, J.; Sarracino, O.; Feng, Y.; Wang, H.; Smith, J. M. Formation of a Cobalt(III) Imido from a Cobalt(II) Amido Complex. Evidence for Proton-Coupled Electron Transfer. *J. Am. Chem. Soc.* **2007**, *129*, 2424−2425. (c) Mehn, M. P.; Brown, S. D.; Jenkins, D. M.; Peters, J. C.; Que, L., Jr Vibrational Spectroscopy and Analysis of Pseudo-tetrahedral Complexes with Metal Imido Bonds. *Inorg. Chem.* **2006**, *45*, 7417−7427. (d) Dai, X.; Kapoor, P.; Warren, T. H. [Me_2NN]Co(η^6-toluene): O = O, N = N, and O = N Bond Cleavage Provides β-Diketiminato Cobalt μ-Oxo and Imido Complexes. *J. Am. Chem. Soc.* **2004**, *126*, 4798−4799. (e) Hu, X.; Meyer, K. Terminal Cobalt(III) Imido Complexes Supported by Tris(Carbene) Ligands: Imido Insertion into the Cobalt−Carbene Bond. *J. Am. Chem. Soc.* **2004**, *126*, 16322−16323. (f) Betley, T. A.; Peters, J. C. Dinitrogen Chemistry from Trigonally Coordinated Iron and Cobalt Platforms. *J. Am. Chem. Soc.* **2003**, *125*, 10782−10783. (g) Jenkins, D. M.; Betley, T. A.; Peters, J. C. Oxidative Group Transfer to Co(I) Affords a Terminal Co(III) Imido Complex. *J. Am. Chem. Soc.* **2002**, *124*, 11238−11239.

(31) (a) Shay, D. T.; Yap, G. P. A.; Zakharov, L. N.; Rheingold, A. L.; Theopold, K. H. Intramolecular C−H Activation by an Open-Shell Cobalt(III) Imido Complex. *Angew. Chem., Int. Ed.* **2005**, *44*, 1508−1510. (b) Thyagarajan, S.; Shay, D. T.; Incarvito, C. D.; Rheingold, A. L.; Theopold, K. H. Intramolecular C−H Activation by Inferred Terminal Cobalt Imido Intermediates. *J. Am. Chem. Soc.* **2003**, *125*, 4440−4441.

(32) (a) King, E. R.; Sazama, G. T.; Betley, T. A. Co(III) Imidos Exhibiting Spin Crossover and C−H Bond Activation. *J. Am. Chem. Soc.* **2012**, *134*, 17858−17861. (b) Baek, Y.; Betley, T. A. Catalytic C−H Amination Mediated by Dipyrrin Cobalt Imidos. *J. Am. Chem. Soc.* **2019**, *141*, 7797−7806. (c) Baek, Y.; Hennessy, E. T.; Betley, T. A. Direct Manipulation of Metal Imido Geometry: Key Principles to Enhance C−H Amination Efficacy. *J. Am. Chem. Soc.* **2019**, *141*, 16944−16953.

(33) Reckziegel, A.; Pietzonka, C.; Kraus, F.; Werncke, C. G. C−H Bond Activation by an Imido Cobalt(III) and the Resulting Amido Cobalt(II) Complex. *Angew. Chem., Int. Ed.* **2020**, *59*, 8527−8531.

(34) Wu, B.; Sánchez, R. H.; Bezpalko, M. W.; Foxman, B. M.; Thomas, C. M. Formation of Heterobimetallic Zirconium/Cobalt Diimido Complexes via a Four-Electron Transformation. *Inorg. Chem.* **2014**, *53*, 10021−10023.

(35) Chomitz, W. A.; Arnold, J. Reactivity of a Co(I) [N_2P_2] complex with azides: evidence for a transient Co(III) imido species. *Chem. Commun.* **2008**, 3648−3650.

(36) (a) Yao, X.-N.; Du, J.-Z.; Zhang, Y.-Q.; Leng, X.-B.; Yang, M.-W.; Jiang, S.-D.; Wang, Z.-X.; Ouyang, Z.-W.; Deng, L.; Wang, B.-W.; Gao, S. Two-Coordinate Co(II) Imido Complexes as Outstanding Single-Molecule Magnets. *J. Am. Chem. Soc.* **2017**, *139*, 373−380. (b) Du, J.; Wang, L.; Xie, M.; Deng, L. A Two-Coordinate Cobalt(II) Imido Complex with NHC Ligation: Synthesis, Structure, and Reactivity. *Angew. Chem., Int. Ed.* **2015**, *54*, 12640−12644.

(37) Liu, Y.; Du, J.; Deng, L. Synthesis, Structure, and Reactivity of Low-Spin Cobalt(II) Imido Complexes [(Me_3P)$_3$Co(NAr)]. *Inorg. Chem.* **2017**, *56*, 8278−8286.

(38) Zhang, L.; Liu, Y.; Deng, L. Three-Coordinate Cobalt(IV) and Cobalt(V) Imido Complexes with N-Heterocyclic Carbene Ligation: Synthesis, Structure, and Their Distinct Reactivity in C−H Bond Amination. *J. Am. Chem. Soc.* **2014**, *136*, 15525−15528.

(39) (a) Goswami, M.; Rebreyend, C.; de Bruin, B. Porphyrin Cobalt(III) "Nitrene Radical" Reactivity; Hydrogen Atom Transfer from *Ortho*-YH Substituents to the Nitrene Moiety of Cobalt-Bound Aryl Nitrene Intermediates (Y = O, NH). *Molecules* **2016**, *21*, 242. (b) Goswami, M.; Lyaskovskyy, V.; Domingos, S. R.; Buma, W. J.; Woutersen, S.; Troeppner, O.; Ivanović-Burmazović, I.; Lu, H.; Cui, X.; Zhang, X. P.; Reijerse, E. J.; DeBeer, S.; van Schooneveld, M. M.; Pfaff, F. F.; Ray, K.; de Bruin, B. Characterization of Porphyrin-Co(III)-'Nitrene Radical' Species Relevant in Catalytic Nitrene Transfer Reactions. *J. Am. Chem. Soc.* **2015**, *137*, 5468−5479. (c) Hopmann, K. H.; Ghosh, A. Mechanism of Cobalt-Porphyrin−Catalyzed Aziridination. *ACS Catal.* **2011**, *1*, 597−600.

(40) van Leest, N. P.; Tepaske, M. A.; Oudsen, J.-P. H.; Venderbosch, B.; Rietdijk, N. R.; Siegler, M. A.; Tromp, M.; van der Vlugt, J. I.; de

https://doi.org/10.1021/acs.organomet.1c00267
Organometallics 2021, 40, 1974−1996

Bruin, B. Ligand Redox Noninnocence in [Co^{III}(TAML)]$^{0/-}$ Complexes Affects Nitrene Formation. *J. Am. Chem. Soc.* **2020**, *142*, 552−563.
(41) van Leest, N. P.; Tepaske, M. A.; Venderbosch, B.; Oudsen, J.-P. H.; Tromp, M.; van der Vlugt, J. I.; de Bruin, B. Electronically Asynchronous Transition States for C−N Bond Formation by Electrophilic [Co^{III}(TAML)]-Nitrene Radical Complexes Involving Substrate-to-Ligand Single-Electron Transfer and a Cobalt-Centered Spin Shuttle. *ACS Catal.* **2020**, *10*, 7449−7463.
(42) Coin, G.; Patra, R.; Rana, S.; Biswas, J. P.; Dubourdeaux, P.; Clémancey, M.; de Visser, S. P.; Maiti, D.; Maldivi, P.; Latour, J.-M. Fe-Catalyzed Aziridination Is Governed by the Electron Affinity of the Active Imido-Iron Species. *ACS Catal.* **2020**, *10*, 10010−10020.
(43) Baek, Y.; Das, A.; Zheng, S.-L.; Reibenspies, J. H.; Powers, D. C.; Betley, T. A. C−H Amination Mediated by Cobalt Organoazide Adducts and the Corresponding Cobalt Nitrenoid Intermediates. *J. Am. Chem. Soc.* **2020**, *142*, 11232−11243.
(44) Bagchi, V.; Kalra, A.; Das, P.; Paraskevopoulou, P.; Gorla, S.; Ai, L.; Wang, Q.; Mohapatra, S.; Choudhury, A.; Sun, Z.; Cundari, T. R.; Stavropoulos, P. Comparative Nitrene-Transfer Chemistry to Olefinic Substrates Mediated by a Library of Anionic Mn(II) Triphenylamido-Amine Reagents and M(II) Congeners (M = Fe, Co, Ni) Favoring Aromatic over Aliphatic Alkenes. *ACS Catal.* **2018**, *8*, 9183−9206.
(45) (a) Jones, M. B.; MacBeth, C. E. Tripodal Phenylamine-Based Ligands and Their Co^{II} Complexes. *Inorg. Chem.* **2007**, *46*, 8117−8119. (b) Çelenligil-Çetin, R.; Paraskevopoulou, P.; Dinda, R.; Staples, R. J.; Sinn, E.; Rath, N. P.; Stavropoulos, P. Synthesis, Characterization, and Reactivity of Iron Trisamidoamine Complexes that Undergo both Metal- and Ligand-Centered Oxidative Transformations. *Inorg. Chem.* **2008**, *47*, 1165−1172. (c) Çelenligil-Çetin, R. *Synthesis, Characterization, and Reactivity of Iron Complexes with N-Donor Ligands in Relation to Oxygenation of Hydrocarbons*, Ph.D. Thesis, Boston University, Boston, MA, 2004.
(46) (a) Paraskevopoulou, P.; Lin, A.; Wang, Q.; Pinnapareddy, D.; Acharrya, R.; Dinda, R.; Çelenligil-Çetin, R.; Floros, G.; Sanakis, Y.; Choudhury, A.; Rath, N. P.; Stavropoulos, P. Synthesis and Characterization of a Series of Structurally and Electronically Diverse Fe(II) Complexes Featuring a Family of Triphenylamido-amine Ligands. *Inorg. Chem.* **2010**, *49*, 108−122. (b) Pinnapareddy, D. *Synthesis and Characterization of Metal Reagents Mediating C−X Activation (X = Cl, H) of Hydrocarbons*, Ph.D. Thesis, University of Missouri−Rolla, Rolla, MO, 2007.
(47) (a) Jones, M. B.; Hardcastle, K. I.; MacBeth, C. E. Synthetic, spectral and structural studies of mononuclear tris(κ^2-amidate) aluminium complexes supported by tripodal ligands. *Polyhedron* **2010**, *29*, 116−119. (b) Jones, M. B.; Hardcastle, K. I.; Hagen, K. S.; MacBeth, C. E. Oxygen Activation and Intramolecular C−H Bond Activation by an Amidate-Bridged Diiron(II) Complex. *Inorg. Chem.* **2011**, *50*, 6402−6404. (c) Villanueva, O.; Weldy, N. M.; Blakey, S. B.; MacBeth, C. E. Cobalt catalyzed sp^3 C−H amination utilizing aryl azides. *Chem. Sci.* **2015**, *6*, 6672−6675.
(48) Bagchi, V.; Raptopoulos, G.; Das, P.; Christodoulou, S.; Wang, Q.; Ai, L.; Choudhury, A.; Pitsikalis, M.; Paraskevopoulou, P.; Stavropoulos, P. Synthesis and characterization of a family of Co(II) triphenylamido-amine complexes and catalytic activity in controlled radical polymerization of olefins. *Polyhedron* **2013**, *52*, 78−90.
(49) Çelenligil-Çetin, R.; Paraskevopoulou, P.; Lalioti, N.; Sanakis, Y.; Staples, R. J.; Rath, N. P.; Stavropoulos, P. Metalloradical Complexes of Manganese and Chromium Featuring an Oxidatively Rearranged Ligand. *Inorg. Chem.* **2008**, *47*, 10998−11009.
(50) (a) Bencini, A.; Benelli, C.; Gatteschi, D.; Zanchini, C. ESR Spectra of Low-Symmetry High-Spin Cobalt(II) Complexes. 2. Pseudotetrahedral Dichlorobis(triphenylphospine oxide)cobalt(II). *Inorg. Chem.* **1979**, *18*, 2137−2140. (b) Benelli, C.; Gatteschi, D. ESR Spectra of Low-Symmetry High-Spin Cobalt(II) Complexes. 10. Five-Coordinated Trigonal-Bipyramidal Complexes. *Inorg. Chem.* **1982**, *21*, 1788−1790. (c) Drulis, H.; Dyrek, K.; Hoffmann, K. P.; Hoffmann, S. K.; Weselucha-Birczynska, A. ESR Spectra of Low-Symmetry Tetrahedral High-Spin Cobalt(II) in a Cinchoninium Tetrachlorocobaltate(II) Dihydrate Single Crystal. *Inorg. Chem.* **1985**, *24*, 4009−4012. (d) Makinen, M. W.; Kuo, L. C.; Yim, M. B.; Wells, G. B.; Fukuyama, J. M.; Kim, J. E. Ground Term Splitting of High-Spin Co^{2+} as a Probe of Coordination Structure. 1. Dependence of the Splitting on Coordination Geometry. *J. Am. Chem. Soc.* **1985**, *107*, 5245−5255. (e) Bennett, B. EPR of Cobalt-Substituted Zinc Enzymes. In *Metals in Biology: Applications of High-Resolution EPR to Metalloenzymes, Biological Magnetic Resonance*; Hanson, G., Berliner, L., Eds.; Springer-Verlag: New York, 2010; Vol. *29*, pp 345−366. (f) Zolnhofer, E. M.; Käß, M.; Khusniyarov, M. M.; Heinemann, F. W.; Maron, L.; van Gastel, M.; Bill, E.; Meyer, K. An Intermediate Cobalt(IV) Nitrido Complex and its N-Migratory Insertion Product. *J. Am. Chem. Soc.* **2014**, *136*, 15072−15078. (g) Antholine, W. E. Resolved Hyperfine at L-band for High-Spin CoEDTA, A Model for Co Sites in Proteins. *Int. J. Mol. Sci.* **2019**, *20*, 2385.
(51) Abragam, A.; Bleaney, B. *Electron Paramagnetic Resonance of Transition Ions*; Clarendon Press: Oxford, 1970.
(52) Pilbrow, J. R. Effective g values for $S = 3/2$ and $S = 5/2$. *J. Magn. Reson.* **1978**, *31*, 479−490.
(53) Petasis, D. T.; Hendrich, M. P. Quantitative Interpretation of Multifrequency Multimode EPR Spectra of Metal Containing Proteins, Enzymes, and Biomimetic Complexes. In *Electron Paramagnetic Resonance Investigations of Biological Systems by Using Spin Labels, Spin Probes, and Intrinsic Metal Ions, Part A*; Qin, P. Z., Warncke, K., Eds.; Methods in Enzymology; Elsevier, 2015; Vol. *563*, Chapter 8, pp 171−208.
(54) Müller, P.; Baud, C.; Jacquier, Y. A Method for Rhodium(II)-Catalyzed Aziridination of Olefins. *Tetrahedron* **1996**, *52*, 1543−1548.
(55) Al-Ajlouni, A.; Espenson, J. H. Epoxidation of Styrenes by Hydrogen Peroxide As Catalyzed by Methylrhenium Trioxide. *J. Am. Chem. Soc.* **1995**, *117*, 9243−9250.
(56) Souto, J. A.; Zian, D.; Muñiz, K. Iodine(III)-Mediated Intermolecular Allylic Amination under Metal-Free Conditions. *J. Am. Chem. Soc.* **2012**, *134*, 7242−7245.
(57) Jiang, X.-K. Establishment and Successful Application of the σ_{JJ}• Scale of Spin-Delocalization Substituent Constants. *Acc. Chem. Res.* **1997**, *30*, 283−289.
(58) Han, H.; Park, S. B.; Kim, S. K.; Chang, S. Copper−Nitrenoid Formation and Transfer in Catalytic Olefin Aziridination Utilizing Chelating 2-Pyridylsulfonyl Moieties. *J. Org. Chem.* **2008**, *73*, 2862−2870.
(59) Liang, S.; Jensen, M. P. Half-Sandwich Scorpionates as Nitrene Transfer Catalysts. *Organometallics* **2012**, *31*, 8055−8058.
(60) Liu, P.; Wong, E. L.-M.; Yuen, A. W.-H.; Che, C.-M. Highly Efficient Alkene Epoxidation and Aziridination catalyzed by Iron(II) Salt + 4,4′,4″-Trichloro-2,2′:6′,2″-terpyridine/4,4″-Dichloro-4′-*O*-PEG-OCH_3-2,2′:6′,2″-terpyridine. *Org. Lett.* **2008**, *10*, 3275−3278.
(61) Dinçtürk, S.; Jackson, R. A. Free radical reactions in solution. Part 7. Substituent effects on free radical reactions: comparison of the σ• scale with other measures of radical stabilization. *J. Chem. Soc., Perkin Trans. 2* **1981**, *2*, 1127−1131.
(62) Jupp, A. R.; Johnstone, T. C.; Stephan, D. W. Improving the Global Electrophilicity Index (GEI) as a Measure of Lewis Acidity. *Inorg. Chem.* **2018**, *57*, 14764−14771.
(63) (a) Johnson, E. R.; Becke, A. D. A post-Hartree−Fock model of intermolecular interactions. *J. Chem. Phys.* **2005**, *123*, No. 024101. (b) Grimme, S.; Ehrlich, S.; Goerigk, L. Effect of the Damping Function in Dispersion Corrected Density Functional Theory. *J. Comput. Chem.* **2011**, *32*, 1456−1465. (c) Grimme, S.; Antony, J.; Ehrlich, S.; Krieg, H. A consistent and accurate ab initio parametrization of density functional dispersion correction (DFT-D) for the 94 elements H-Pu. *J. Chem. Phys.* **2010**, *132*, 154104.
(64) (a) Lu, X.; Li, X.-X.; Lee, Y.-M.; Jang, Y.; Seo, M. S.; Hong, S.; Cho, K.-B.; Fukuzumi, S.; Nam, W. Electron-Transfer and Redox Reactivity of High-Valent Iron Imido and Oxo Complexes with the Formal Oxidation States of Five and Six. *J. Am. Chem. Soc.* **2020**, *142*, 3891−3904. (b) Sabenya, G.; Gamba, I.; Gómez, L.; Clémancey, M.; Frisch, J. R.; Klinker, E. J.; Blondin, G.; Torelli, S.; Que, L., Jr.; Martin-Diaconescu, V.; Latour, J.-M.; Lloret-Fillol, J.; Costas, M. Octahedral

https://doi.org/10.1021/acs.organomet.1c00267
Organometallics 2021, 40, 1974−1996

iron(iv)−tosylimido complexes exhibiting single electron-oxidation reactivity. *Chem. Sci.* **2019**, *10*, 9513−9529. (c) Hong, S.; Lu, X.; Lee, Y.-M.; Seo, M. S.; Ohta, T.; Ogura, T.; Clémancey, M.; Maldivi, P.; Latour, J.-M.; Sarangi, R.; Nam, W. Achieving One-Electron Oxidation of a Mononuclear Nonheme Iron(V)-Imido Complex. *J. Am. Chem. Soc.* **2017**, *139*, 14372−14375. (d) Kumar, S.; Faponle, A. S.; Barman, P.; Vardhaman, A. K.; Sastri, C. V.; Kumar, D.; de Visser, S. P. Long-range Electron Transfer Triggers Mechanistic Differences between Iron(IV)-Oxo and Iron(IV)-Imido Oxidants. *J. Am. Chem. Soc.* **2014**, *136*, 17102−17115.

(65) (a) Ogliaro, F.; Harris, N.; Cohen, S.; Filatov, M.; de Visser, S. P.; Shaik, S. A Model "Rebound" Mechanism of Hydroxylation by Cytochrome P450: Stepwise and Effectively Concerted Pathways, and Their Reactivity Patterns. *J. Am. Chem. Soc.* **2000**, *122*, 8977−8989. (b) Shaik, S.; de Visser, S. P.; Ogliaro, F.; Schwarz, H.; Schröder, D. Two-state reactivity mechanisms of hydroxylation and epoxidation by cytochrome P-450 revealed by theory. *Curr. Opin. Chem. Biol.* **2002**, *6*, 556−567. (c) Moreau, Y.; Chen, H.; Derat, E.; Hirao, H.; Bolm, C.; Shaik, S. NR Transfer Reactivity of Azo-Compound I of P450. How Does the Nitrogen Substituent Tune the Reactivity of the Species toward C−H and C═C Activation? *J. Phys. Chem. B* **2007**, *111*, 10288−10299.

(66) (a) Kuijpers, P. F.; van der Vlugt, J. I.; Schneider, S.; de Bruin, B. Nitrene Radical Intermediates in Catalytic Synthesis. *Chem. - Eur. J.* **2017**, *23*, 13819−13829. (b) Xiong, T.; Zhang, Q. New amination strategies based on nitrogen-centered radical chemistry. *Chem. Soc. Rev.* **2016**, *45*, 3069−3087.

(67) (a) Xiong, P.; Xu, H.-C. Chemistry with Electrochemically Generated N-Centered Radicals. *Acc. Chem. Res.* **2019**, *52*, 3339−3350. (b) Wang, P.; Zhao, Q.; Xiao, W.; Chen, J. Recent advances in visible-light photoredox-catalyzed nitrogen radical cyclization. *Green Synth.Catal.* **2020**, *1*, 42−51. (c) Zheng, S.; Gutiérrez-Bonet, Á.; Molander, G. A. Merging Photoredox PCET with Ni-Catalyzed Cross-Coupling: Cascade Amidoarylation of Unactivated Olefins. *Chem.* **2019**, *5*, 339−352. (d) Davies, J.; Svejstrup, T. D.; Reina, D. F.; Sheikh, N. S.; Leonori, D. Visible-Light-Mediated Synthesis of Amidyl Radicals: Transition-Metal-Free Hydroamination and *N*-Arylation Reactions. *J. Am. Chem. Soc.* **2016**, *138*, 8092−8095.

(68) Wang, Q.; Wang, P.; Gao, X.; Wang, D.; Wang, S.; Liang, X.; Wang, L.; Zhang, H.; Lei, A. Regioselective/electro-oxidative intermolecular [3 + 2] annulation for the preparation of indolines. *Chem. Sci.* **2020**, *11*, 2181−2186.

(69) (a) Usharani, D.; Janardanan, D.; Li, C.; Shaik, S. A Theory for Bioinorganic Chemical Reactivity of Oxometal Complexes and Analogous Oxidants: The Exchange and Orbital-Selection Rules. *Acc. Chem. Res.* **2013**, *46*, 471−482. (b) Swart, M.; Gruden, M. Spinning around in Transition-Metal Chemistry. *Acc. Chem. Res.* **2016**, *49*, 2690−2697.

(70) Ren, Y.; Cheaib, K.; Jacquet, J.; Vezin, H.; Fensterbank, L.; Orio, M.; Blanchard, S.; Desage-El Murr, M. Copper-Catalyzed Aziridination with Redox-Active Ligands: Molecular Spin Catalysis. *Chem. - Eur. J.* **2018**, *24*, 5086−5090.

(71) Schümann, J. M.; Wagner, J. P.; Eckhardt, A. K.; Quanz, H.; Schreiner, P. R. Intramolecular London Dispersion Interactions Do Not Cancel in Solution. *J. Am. Chem. Soc.* **2021**, *143*, 41−45.

(72) (a) Rösel, S.; Becker, J.; Allen, W. D.; Schreiner, P. R. Probing the Delicate Balance between Pauli Repulsion and London Dispersion with Triphenylmethyl Derivatives. *J. Am. Chem. Soc.* **2018**, *140*, 14421−14432. (b) Rösel, S.; Balestrieri, C.; Schreiner, P. R. Sizing the role of London dispersion in the dissociation of all-*meta tert*-butyl hexaphenylethane. *Chem. Sci.* **2017**, *8*, 405−410. (c) Grimme, S.; Schreiner, P. R. Steric Crowding Can Stabilize a Labile Molecule: Solving the Hexaphenylethane Riddle. *Angew. Chem., Int. Ed.* **2011**, *50*, 12639−12642.

(73) (a) Bursch, M.; Caldeweyher, E.; Hansen, A.; Neugebauer, H.; Ehlert, S.; Grimme, S. Understanding and Quantifying London Dispersion Effects in Organometallic Complexes. *Acc. Chem. Res.* **2019**, *52*, 258−266. (b) Grimme, S.; Huenerbein, R.; Ehrlich, S. On the Importance of the Dispersion Energy for the Thermodynamic Stability of Molecules. *ChemPhysChem* **2011**, *12*, 1258−1261.

(74) (a) Power, P. P. An Update on Multiple Bonding between Heavier Main Group Elements: The Importance of Pauli Repulsion, Charge-Shift Character, and London Dispersion Force Effects. *Organometallics* **2020**, *39*, 4127−4138. (b) Liptrot, D.; Power, P. P. London dispersion forces in sterically crowded inorganic and organometallic molecules. *Nat. Rev. Chem.* **2017**, *1*, No. 0004.

(75) Wagner, J. P.; Schreiner, P. R. London Dispersion in Molecular Chemistry − Reconsidering Steric Effects. *Angew. Chem., Int. Ed.* **2015**, *54*, 12274−12296.

https://doi.org/10.1021/acs.organomet.1c00267
Organometallics 2021, 40, 1974−1996